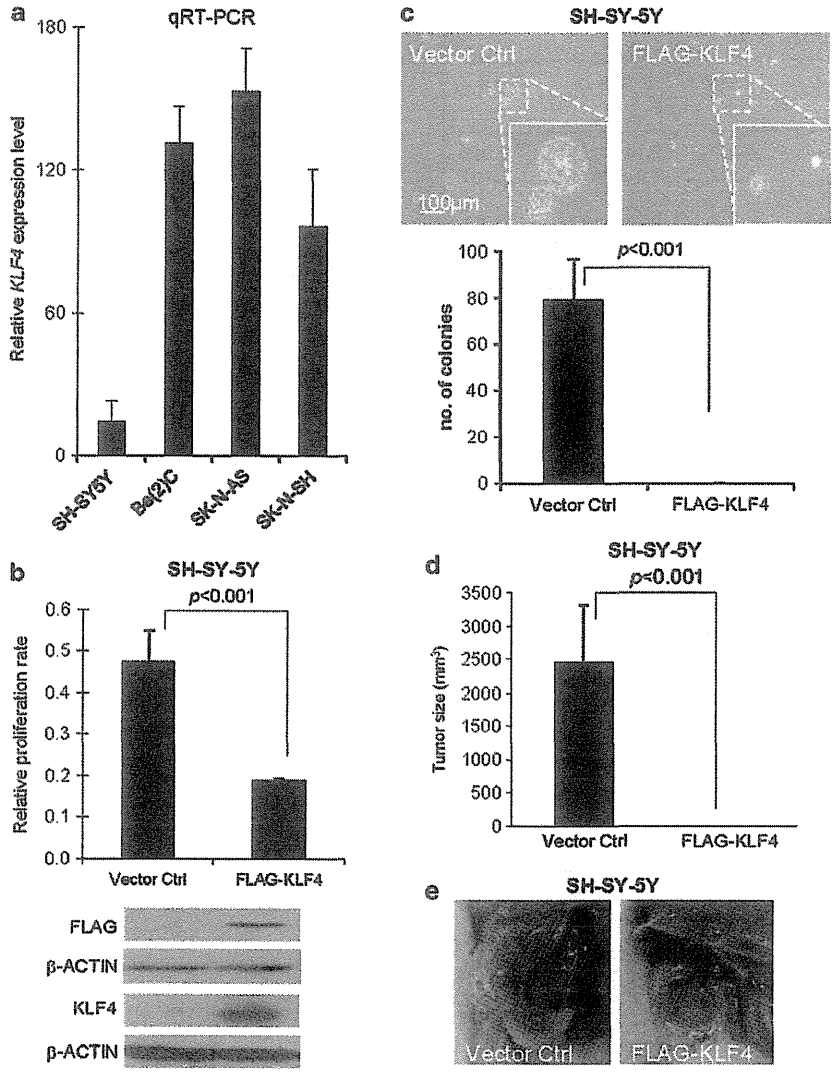

Figure 2. Effect of KLF4 overexpression on NB cell growth and tumorigenicity. **(a)** Expression of *KLF4* in various NB cell lines was measured by real-time reverse transcription-PCR (RT–PCR). *KLF4* expression was normalized to that of *18S* mRNA. **(b)** Upper panel: BrdU incorporation assays on the SH-SY-5Y cells stably transfected with FLAG-KLF4 and empty vector. Lower panel: Immunoblot analysis of the expression of FLAG-KLF4 in the stable KLF4 overexpressing transfectant, and the vector control clone with anti-FLAG or anti-KLF4 antibodies. Blots were stripped and reprobed for β-actin expression to ensure equal protein loading. **(c)** The anchorage independency of the stable transfectants was tested using soft agar assay. Upper panel: Pictures were taken at week 6 of the culture. Lower panel: Quantitative analysis on number of colonies detected in each group. **(d, e)** Effect of KLF4 on tumorigenesis was examined using KLF4 overexpressing stable transfectants and the vector control clone in SCIB/Beige mice. **(d)** Cells were injected subcutaneously into the flank of each mouse. No tumor was observed from the KLF4 overexpressing group and tumor volumes in mice from the control group were measured. Data represent the mean tumor volume for four mice (Bars, 95% CIs, Student's *t*-test). **(e)** SH-SY-5Y stable transfectants were injected orthotropically into adrenal fat pad of each mouse. Mice were killed at 2 months ($n=4$) or 100 days ($n=3$) after injection and tumors were observed in the control group, but not in the KLF4 overexpressing group. A representative picture of mice killed at day100 is shown. The values reported in the bar graphs represent the mean ± 95% CIs from three independent assays, each in triplicate. Data were analyzed by two-sided unpaired Student's *t*-tests, and *P*-values <0.05 were considered to be statistically significant.

clones were treated with retinoic acid for 4 weeks. The neuronal differentiation was then monitored by the presence of neurite outgrowth. Four weeks after treatment, both control and knock-down clones could generate neurite outgrowth at a similar extent (Figure 4e), suggesting that KLF4 may not directly contribute to the neuronal differentiation of NB cells.

KLF4 upregulates $p21^{WAF1/CIP1}$ expression, but not p53 in NB cells

Given that KLF4 has been shown to upregulate the CDK2 inhibitor $p21^{WAF1/Cip1}$ and repress p53 suppressor to induce growth arrest, we then examined if KLF4 mediates the expression of these two cell-cycle regulators in NB cells. As revealed by western blot analysis, elevated expression of $p21^{WAF1/Cip1}$ was observed in the KLF4 overexpressing clone (FLAG-KLF4), while CYCLIN D2 was substantially downregulated in these cells (Figure 5b). Nevertheless, p53 expression was not affected (Figure 5a).

To test whether KLF4 upregulates $p21^{WAF1/Cip1}$ expression by direct activation of gene transcription, we transfected SK-N-AS cells with a plasmid encoding firefly luciferase under the control of a $p21^{WAF1/CIP1}$ (p21-Luc) or p53 (p53-Luc) promoters, expression vectors for wild-type KLF4 or KLF4 mutant with partial deletion on

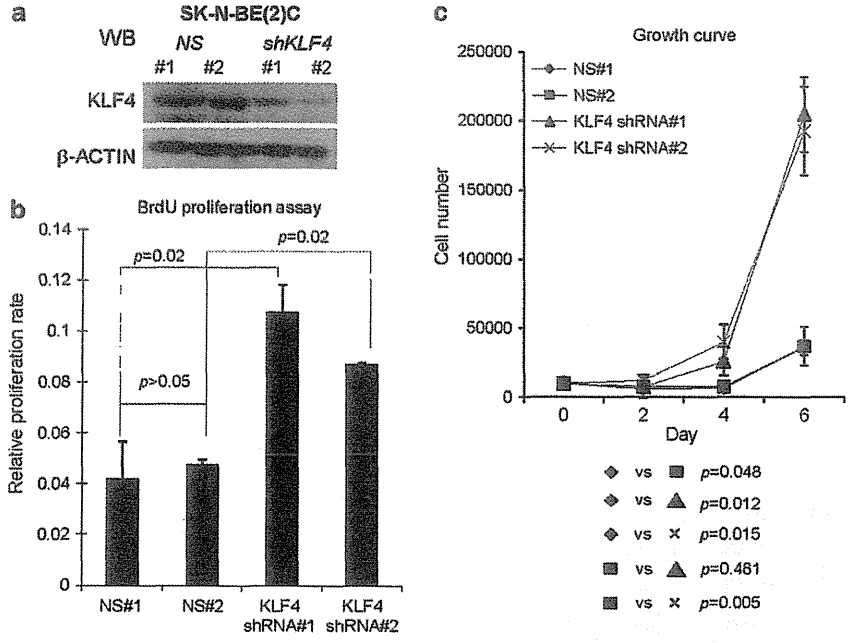

Figure 3. Effect of KLF4 knockdown on NB cell. (**a**) Western blot analysis of the expression of *KLF4* in the *KLF4* stable knockdown clones and the non-silencing control clones. (**b**) BrdU incorporation assays on BE(2)C cells stably transduced with non-silencing control (NS#1 and 2) and *shKLF4* (shKLF4#1 and 2). The values reported in the bars represent the mean of samples ± 95% CIs. (**c**) Growth curves were performed by plating a fixed number of cells and counting cells at different time points. The mean cell numbers of triplicates from one experiment are shown (Bars, 95% CIs, Student's *t*-test). All experiments were repeated three times and each in triplicate. Data were analyzed by two-sided unpaired Student's *t*-tests, and *P*-values <0.05 were considered to be statistically significant.

activation domain (KLF4ΔA) or KLF4 mutant with a complete deletion of DNA-binding domain (KLF4ΔDBD), or the control empty vector (pFLAG-CMV), and a plasmid encoding Renilla luciferase (pRL-SV40). The extents to which KLF4 and its mutants transactivated the $p21^{WAF1/CIP1}$ and p53 promoters were assessed by normalizing firefly luciferase activity to Renilla luciferase activity. Overexpression of KLF4 significantly activated $p21^{WAF1/CIP1}$ transcription, while its transactivity has been partially or completely abolished when the activation domain or DNA-binding domain was deleted, respectively (Figure 5c). In contrast, there is no transactivation activity detected with the p53 reporter (Figure 5c). This finding is consistent with the western blot data, suggesting that KLF4 directly upregulates $p21^{WAF1/CIP1}$, but not p53. Importantly, knocking down $p21^{WAF1/CIP1}$ in the KLF4 overexpressing cells could significantly increase the proliferation rate of these cells, suggesting that $p21^{WAF1/CIP1}$ is implicated in the KLF4 mediated growth suppression (Figure 5d).

In NB, p53 is mainly implicated in regulation of apoptosis. To address if tumor suppressive effect of KLF4 also relies on p53 induced apoptosis, an NB line, SK-N-AS, of exon 9 deletion in the *p53* gene was used. Annexin V apoptosis assay revealed that overexpression of KLF4 could significantly (but slightly) induce apoptosis of SK-N-AS ($P=0.044$), whereas transfection with KLF4ΔA or KLF4ΔDBD expression construct did not increase apoptotic cells in the culture (Figure 5e). It is noteworthy that similar result was observed with SH-SY-5Y, which carries the wild-type p53 (Supplementary Figure 1).

In regard to cell growth, overexpression of KLF4 could profoundly inhibit cell growth of SK-N-AS as indicated in the colony formation assay. Overexpression of wild-type KLF4, but not the mutants (KLF4ΔA and KLF4ΔDBD) resulted in a dramatic reduction in number as well as the size of colonies obtained (Figure 5f). In concordance with these observations, transient knockdown of *KLF4* in SK-N-SH cells that express wild-type p53 also significantly promoted the cell growth as indicated in the proliferation assay (Figure 5g). Therefore, all these data suggest that $p21^{WAF1/CIP1}$-dependent growth retardation may represent one of the predominant mechanisms by which KLF4 inhibits NB cell growth.

Dysregulation of transforming growth factor β and cell-cycle pathways in KLF4 overexpressing NB cells

To further delineate the underlying molecular pathways implicated in KLF4 induced fibromuscular differentiation and retarded growth of NB cells, global gene expression profiles of SH-SY-5Y cells stably transfected with pFLAG-CMV-KLF4 (FLAG-KLF4) or pFLAG-CMV (Ctrl) construct were compared. The microarray analysis revealed that 11 448 genes are differentially expressed ($P<0.01$) in KLF4 overexpressing and control clones. Seventy-three percent of these genes showed greater than twofold changes in either direction, 35.3 and 24.8% were found to be upregulated and downregulated, respectively. Subsequent pathway-based analysis further identified that transforming growth factor beta (TGFβ) pathway genes are highly dysregulated in the KLF4 overexpressing cells (Figure 6a; Tables 3 and 4). They included TGFβ receptors (*TGFBR1, 2* and *3*), its signal transducer (*SMAD 2, 3, 4, 5, 6, 7, 9*), co-factor (*LEF1* and *ZNF423*), repressor (*ZFHX1B*) and effector genes (*SERPINE1* and *SKIL*). In addition, two key myogenic regulators (myocyte enhancer factor 2, *MEF2*; myogenic differentiation 1, *MYOD1*) and fibromuscular differentiation markers (*S100* and *SM22*) were found upregulated in KLF4 overexpressing SH-SY-5Y. Calcium calmodulin-dependent protein kinase (*CAMK2*), an upstream regulator for MEF2, was also elevated.

In regard to cell-cycle progression, elevated expression of $p21^{WAF1/CIP1}$ (2.4-folds) and cell-cycle checkpoint kinase (*ATM*, 2.9-folds) and repression of mitotic check point regulators (*CDC20* and *hBUBR1*) were also detected in the KLF4 overexpressing cells, accounting for the retarded cell growth (Figure 6b).

In summary, overexpression of KLF4 in SH-SY-5Y cells altered both TGFβ and cell-cycle pathway genes. In particular, the specific composition of TGFβ-induced SMAD transcription factor complexes seems to be an important determinant to turn on the myogenic regulators (*MEF2A* and *MYOD1*), promoting fibromuscular differentiation of NB cells. In parallel, dysregulation

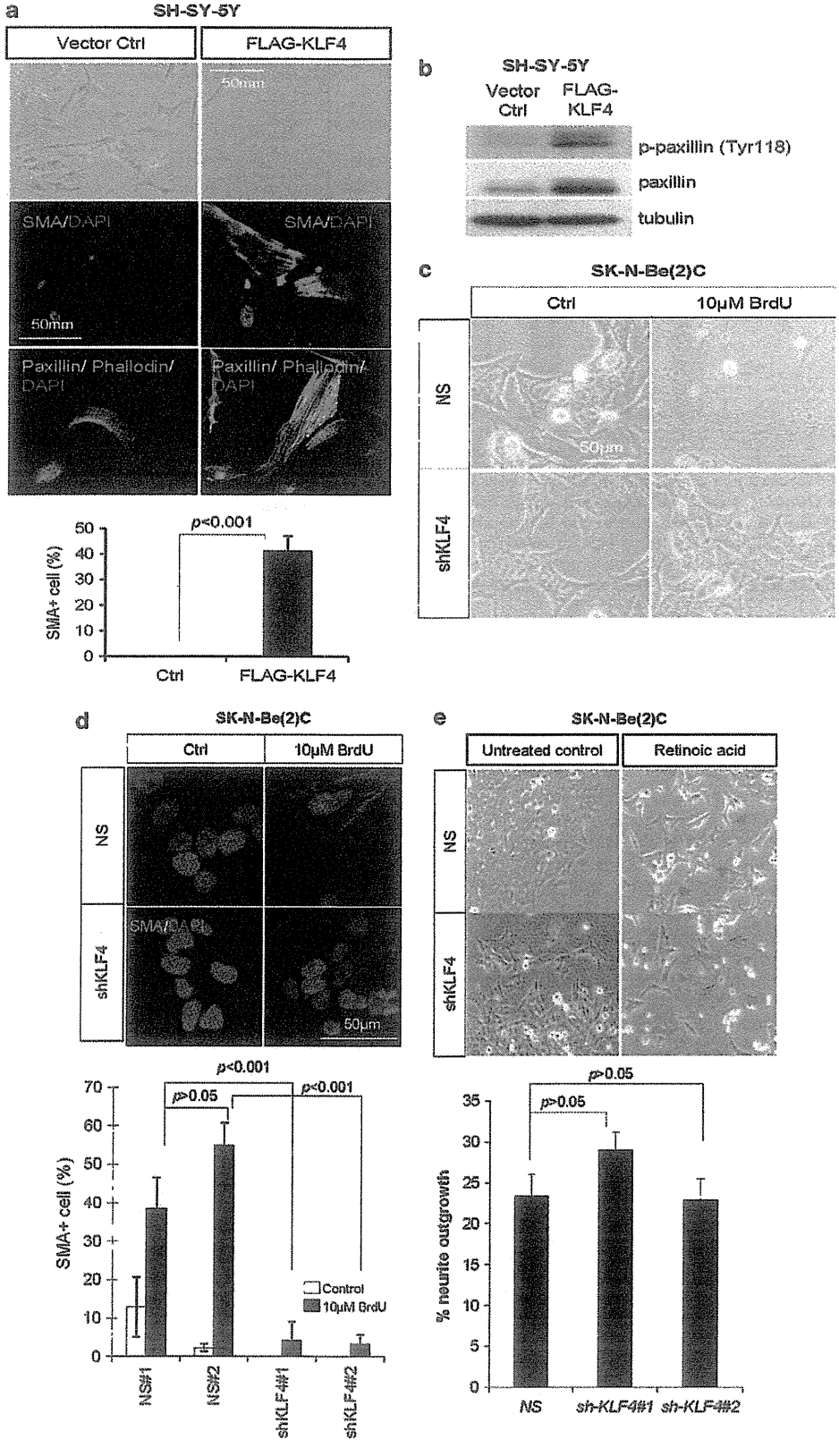

of cell-cycle pathway genes ($p21^{WAF1/CIP1}$ and *CDC20*) may lead to retarded cell growth (Figure 6c).

DISCUSSION

The bipotent plasticity of NB cells to neuronal and fibromuscular lineages is believed to account for the diverse clinical outcomes of NB.[22,23,42–45] As the bipotent progenitor cells possess high clonogenicity, they would generate a vast population of neuronal committed cells and contribute to the bulk tumor. On the other hand, if these NB cells differentiate to fibromuscular cells, then it may result in tumor regression. Therefore, genetic alternations that favor NB progenitors to differentiate toward neuroblastic lineage may promote tumor progression, while to fibromuscular lineage may lead to a favorable clinical outcome.

In this study, we demonstrated that *KLF4* represents a favorable gene for NB and loss of *KLF4* expression is usually associated with poor prognosis, particularly in the high-risk patient of age older than 1 year, low *TRKA* expression or with *MYCN* amplification. Cox regression model further suggested that *KLF4* expression, *TRKA* expression, metastasis and *MYCN* amplification status contribute independent predictive power in determining tumor outcome. Indeed, our functional data also indicated that KLF4 may function independent of these pathways. Overexpression of KLF4 in SH-SY-5Y cells induced morphological change of the cells accompanied by upregulation of focal adherent protein (paxillin). Nevertheless, these changes did not alter the cell motility. With transwell migration assay, we found that the KLF4 overexpressing SH-SY-5Y and the control clones exhibit similar motility (Supplementary Figure 2). In addition, expression profiling analysis on a panel of NB cell lines also revealed that there is no obvious association between *KLF4* and *MYCN* expression (Supplementary Figure 3). MYCN has been shown to directly suppress *TRKA* expression, but suppressive effect of MYCN on KLF4 expression was not observed. Using the Tet21N(–) NB cells that harbor a tetracycline-inducible *MYCN* transgene,[46] we found that tetracycline induced overexpression of MYCN did not alter KLF4 expression (Supplementary Figure 4), indicating that MYCN does not directly regulate KLF4 expression.

On the other hand, we demonstrated that KLF4 reduces NB cell growth, mediates terminal differentiation to fibromuscular lineage and the cell-cycle progression as well as induces apoptosis of NB cells. Here, we used four NB cell lines representing neuroblastic (SH-SY-5Y, N-type), fibromuscular (SK-N-AS, S-type), stem cell-like (BE(2)C, I-type) and mixed (SK-N-SH, mixed) populations of NB to elucidate how KLF4 may affect different cell compartments of NB and contribute to good prognosis. Despite SH-SY-5Y comprises majority of neuroblastic cells, previous subcloning studies indicated it also contains a small population of bipotent progenitors, representing an excellence experimental model for NB. Dynamic interconversion between different cell subpopulations has also been demonstrated, the progenitors provide an indefinite replenishment of the neuroblastic bulk population, whereas they also rely on the neuroblastic cells for their maintenance. Removal of the neuroblastic sub-population will purge the progenitors and induce their terminal commitment to the fibromuscular phenotypes, resulting in spontaneous regression of NB.[23] When we stably overexpressed KLF4 in SH-SY-5Y, all the KFL4 expressing transfectants exhibited an epithelial-like phenotypes and some even expressed fibromuscular marker. Importantly, these cells were totally non-tumorigenic *in vivo*. These observations prompted us to speculate if (i) KLF4 overexpression induces apoptosis of neuroblastic cell compartments and indirectly drive progenitors toward to fibromuscular differentiation; (ii) stable change in KLF4 expression favors the outgrowth of a minority population; or (iii) KLF4 has an active role to direct fibromuscular differentiation. To address this question, the apoptotic potential of KLF4 was tested. Our data from Annexin V apoptosis and growth assays indicated that KLF4 indeed can slightly induce apoptosis, while its inhibitory effect on cell growth mainly relied on the upregulation of $p21^{WAF1/CIP1}$ expression in SH-SY-5Y and SK-N-AS cells. Knocking down $p21^{WAF1/CIP1}$ could partially rescue the suppressive function of KLF4 in cell proliferation. In line with these observations, knockdown of KLF4 in BE(2)C and SK-N-SH significantly promoted cell growth *in vitro*, but loss of KLF4 was not sufficient to induce tumor. Given that KLF4 exhibited similar suppressive function in NB cells containing either wild-type (SH-SY-5Y) or mutant (BE(2)C and SK-N-AS) p53, it further suggests that p53-driven apoptosis is unlikely the only mechanism by which KLF4 inhibits NB cell growth.

In regards to NB differentiation, KLF4 knockdown robustly abolished the differentiation plasticity of BE(2)C cells to commit to fibromuscular lineage, implying that KLF4 is critical for fibromuscular lineage differentiation. Despite we cannot completely rule out the possibility that KLF4 induced fibromuscular differentiation is a secondary effect of a biased selection process, with our current data and data previously published by others,[37] we believe that KLF4 is likely taking an active role in this cellular process. In particular, TGFβ has been shown to induce smooth muscle cell differentiation of a non-cancerous neural crest cell line, through modulating SMAD, mitogen-activated protein kinase, phosphoinositol-3 kinase and RhoA signalings.[47] Our global gene expression profiling data also showed that TGFβ pathway has been highly dysregulated in NB cells upon overexpression of KLF4, they include the TGFβ receptors, various *SMAD* and their effector genes. Moreover, other signaling modulators implicated in smooth muscle lineage differentiation, such as MAPK (*MAPK9*), calcium (*CAMK2*) signalings were also found upregulated. CAMK2 is known to phosphorylate a series of conserved serine residue on class II histone deacetylases and promote the nuclear-to-cytoplasmic shuttling of these histone deacetylases and the subsequent activation of MEF2, in turn, induce fibromuscular

Figure 4. Effect of KLF4 on fibromuscular lineage differentiation of NB. (**a**) Bright field of SH-SY-5Y cells stably transfected with empty vector and FLAG-KLF4 expression construct. The magnification of the pictures is ×200 (scale bar = 50 μm). Expression of SMA and paxillin was detected using immunocytochemistry. The F-actin was visualized by TRITC-labeled phalloidin. Cells were counterstained with DAPI. The magnification of the pictures is ×400 (scale bar = 50 μm). The percentages of SMA^+ cells in the stable transfectants are shown in the bar graph (Bars, 95% CIs, Student's *t*-test). (**b**) Protein lysates were obtained from the control and KLF4 overexpressing clones. The expression of pTry118-paxillin and total paxillin was detected by western blotting. Tubulin expression served as loading controls. (**c**) BE(2)C cells stably transduced with lentivirus expressing non-silencing *shRNA* and *shKLF4* were cultured in medium with or without BrdU (10 μM). Two weeks after induction, morphological changes of the cells were observed under the microscope. Representative pictures from each group are shown. The magnification of the pictures is ×400 (scale bar = 50 μm). (**d**) Expression of fibromuscular marker, SMA was detected using immunocytochemistry. Upper panel: Representative pictures from each group are shown. The magnification of the pictures is ×400 (scale bar = 50 μm). Lower panel: Data represent the mean of SMA-positive cells in each group. (**e**) BE(2)C control and knockdown clones were cultured in medium with or without retinoic acid (1 μM). Four weeks after induction, the presence of neurite outgrowth of these cells was observed under the microscope. Upper panel: Representative pictures from each group are shown. Lower panel: Quantitative data represent percentage of cells with neurite outgrowth in each group. Values reported in the graphs represent the mean ± 95% CIs from three independent assays, each in triplicate. Data were analyzed by two-sided unpaired Student's *t*-tests, and *P*-values <0.05 were considered to be statistically significant.

differentiation.[48,49] Given that TGFβ-SMAD pathways have been implicated in many biological processes and varied signaling pathways are upregulated in KLF4 overexpressing cells, it is conceivable that multiple pathways with a specific composition of various pathway genes are crucial for the smooth muscle differentiation. Noteworthy, our data suggest that two myogenic modulators, *MEF2* and *MYOD1*, are likely the common downstream targets of these pathways for the activation of fibromuscular

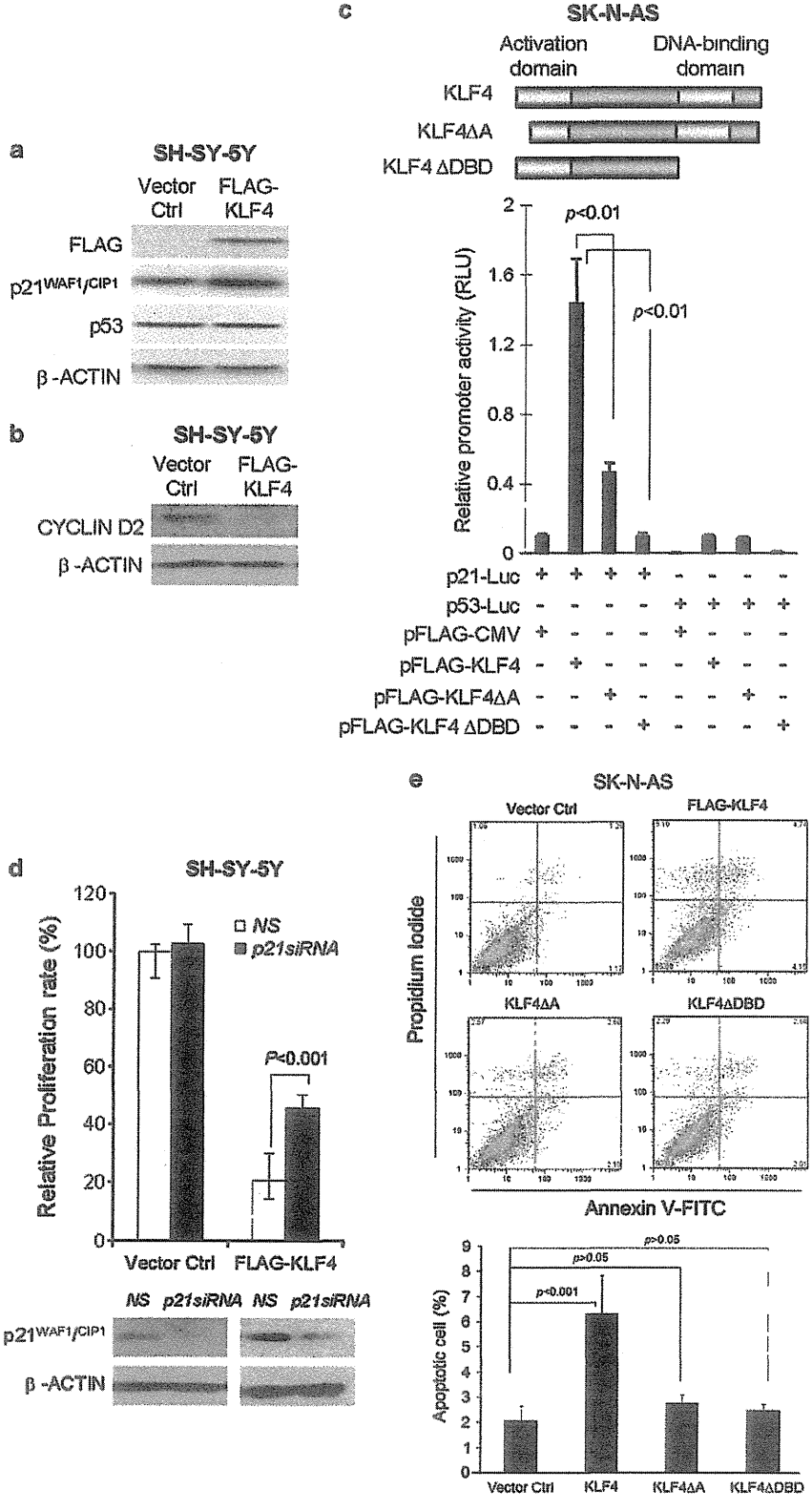

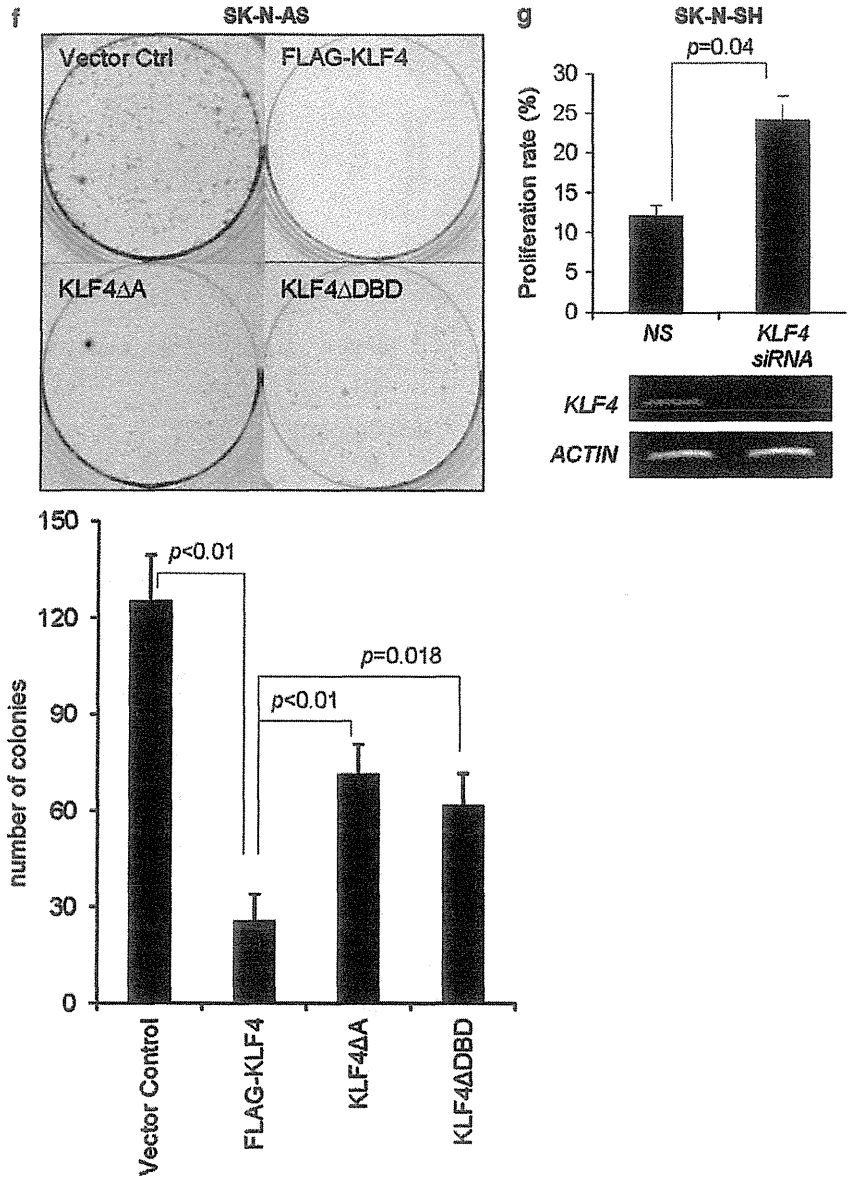

Figure 5. Continued.

Figure 5. Effect of KLF4 on apoptosis and cell growth. (**a**, **b**) Expression of $p21^{WAF1/CIP1}$, p53 and CYCLIN D2 in KLF4 overexpressing SH-SY-5Y and vector control stable transfectants were detected by western blotting. β-Actin expression served as loading controls. (**c**) Comparison of wild-type KLF4, KLF4ΔA and KLF4ΔDBD transactivation of $p21^{WAF1/CIP1}$ and p53 enhancers. Schematic diagram summarizes the expression constructs for the wild-type KLF4 and KLF4 deletion mutants. KLF4ΔA bears a partial deletion of the activation domain and KLF4ΔDBD has a complete deletion of the DNA-binding domain (DBD). Reporter plasmids encoding luciferase under the control of $p21^{WAF1/CIP1}$ and p53 enhancers, p21-Luc and p53-Luc, respectively, were transfected into SK-N-AS along with an internal control plasmid encoding Renilla luciferase pRL-SV40, and either a plasmid encoding wild-type KLF4 (pFLAG-KLF4), KLF4ΔA (pFLAG-KLF4ΔA), KLF4ΔDBD (pFLAG-KLF4ΔDBD) or empty vector (pFLAG-CMV). Promoter activity is expressed as relative luciferase activity after normalization to Renilla activity. (**d**) Annexin V apoptosis assay. (**e**) SK-N-AS cells were transiently transfected with empty vector (pFLAG-CMV), KLF4 (pFLAG-KLF4), KLF4ΔA (pFLAG-KLF4ΔA) or KLF4ΔDBD (pFLAG-KLF4ΔDBD). The late apoptotic cells (Annexin V and propidium iodide double positive) were quantified using flow cytometry. (**f**) Colony formation assay. SK-N-AS cells transiently transfected with empty vector, wild-type or mutant KLF4 expression constructs were plated at the same density and grown in selection medium for 2 weeks. Colonies were stained and photographed. Representative pictures from each group were shown. The experiments were repeated three times with triplicate. Lower panel: Quantitative data are shown, (**g**) Upper panel: BrdU incorporation assays on the SK-N-SH cells transfected with non-silencing siRNA (NS) and KLF4 siRNA (siKLF4). Lower panel: RT–PCR analysis of the expression of *KLF4* in the *siKLF4* and non-silencing *siRNA* transfected cells. The values reported in the bar graphs represent the mean ± 95% CIs from three independent assays, each in triplicate. Data were analyzed by two-sided unpaired Student's *t*-tests, and *P*-values <0.05 were considered to be statistically significant. A full colour version of this figure is available at the *Oncogene* journal online.

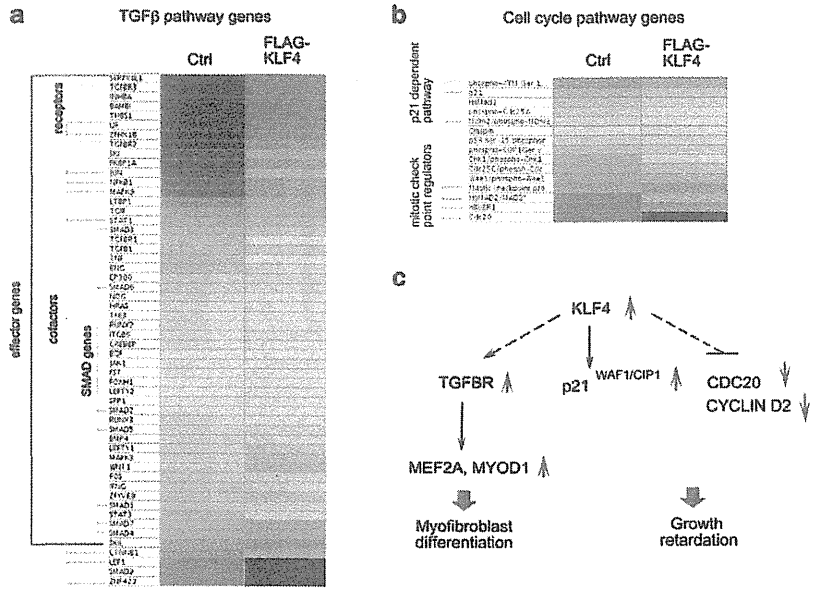

Figure 6. Dysregulation of TGFβ and cell-cycle pathway genes in KLF4 overexpressing SH-SY-5Y cells. Heatmaps showing (**a**) TGFβ, (**b**) cell-cycle pathway genes have been differentially regulated by KLF4. Blue cells denote low expression, red cells denote high expression and yellow cells denote intermediate expression. Microarray experiments were performed in triplicates using Human Genome U133 Plus 2.0 GeneChip from Affymetrix, and *P*-values smaller than 0.01 were considered to be statistically significant, genes with fold changes larger than two (cutoff: fold change >2) were included for the pathway analyses. (**c**) Schematic overview of the roles of TGFβ and cell-cycle regulators in KLF4 induced fibromuscular differentiation and growth retardation of NB cells (dashed line: unknown mechanism).

Table 3. TGF pathway genes upregulated in KLF4 overexpressing SH-SY-5Y

Gene symbol	*Entrez gene*	*Fold change*
S100A10	6281	204.7
S100A11	6282	140.3
THBS1	7057	46.9
SERPINE1	5054	29.8
TGFBR3	7049	15.9
TGFBR3	7049	10.7
ZEB2	9839	9.2
BAMBI	25 805	7.3
TGFBR2	7048	7.0
MEF2A	4205	4.0
LIF	3976	3.8
STAT1	6772	3.4
JUN	3725	3.0
CAMK2	817	3.0
FKBP1A	2280	2.9
SM22	10 618	2.6
MYOD1	4642	2.6
INHBA	3624	2.4
MAPK9	5601	2.3
NFKB1	4790	2.1
LTBP1	4052	2.1
SMAD6	4091	2.0

Abbreviations: KLF4, Krüppel-like factor 4; TGF, transforming growth factor. Genes implicated in myofibroblast differentiation are bolded.

Table 4. TGF pathway genes downregulated in KLF4 overexpressing SH-SY-5Y

Gene symbol	*Entrez gene*	*Fold change*
LEF1	51 176	62.7
ZNF423	23 090	14.4
PRKAR1A	5573	11.6
SMAD4	4089	6.3
PRKAR2B	5577	6.0
CTNNB1	1499	5.4
SKIL	6498	5.1
PRKACB	5567	4.6
ZEB1	6935	3.7
EZH2	2146	2.2

Abbreviations: KLF4, Krüppel-like factor 4; TGF, transforming growth factor. Genes implicated in myofibroblast differentiation are bolded.

differentiation of NB cells. In parallel, KLF4 also directly or indirectly alters a panel of cell-cycle mediators (*p21$^{WAF1/CIP1}$*, *CDC20*, *CYCLIN D2*, and so on), which may lead to retarded cell growth.

Taken together, high KLF4 expression may favor tumor regression through inducing cell-cycle arrest and fibromuscular lineage differentiation, while KLF4-deficient NB progenitors may maintain a neuroblastic bias over the KLF4 expressing counterparts. Loss of KLF4 may also promote the growth of neuroblastic cells and account for the poor prognosis. Nevertheless, whether KLF4 induced growth retardation and fibromuscular differentiation represent two divergent processes or a coordination between these two cellular processes is required for inducing NB regression remains unclear.

In summary, we have demonstrated that KLF4 is a favorable gene in NB. Integrated analysis on the expression pattern of KLF4 with other key prognostic markers might further enhance its prognostic value for the prediction of clinical outcome of the tumors and facilitate patient stratification. In addition, our functional studies directly provide a mechanistic explanation on how KLF4 may contribute to the favorable clinical outcome and highlight the importance of two distinctive cellular processes, proliferation and differentiation, in determining the tumor behavior.

MATERIALS AND METHODS

Primary NB tumor samples

A total of 102 NB tumor specimens obtained from the Chiba Cancer Center Research Institute, Chiba, Japan, were included in this study. All subjects were unrelated ethnic Japanese and recruited in Japan between 1995 and 2003. Patients were treated by the standard protocols.[50,51] The median age of the entire cohort was 19.5 months (range: 0–163 months). Tumors at all stages were included: Stage 1, $n=27$, 26.5%; Stage 2, $n=15$, 14.7%; Stage 3, $n=32$, 31.4%; Stage 4, $n=23$, 22.5%; Stage 4S, $n=5$, 4.9%. All tumors were histopathologically diagnosed as NB and were staged according to the International Neuroblastoma Staging System.[3] *MYCN* copy number, *TRKA* mRNA expression and DNA ploidy were measured as reported previously.[52] Informed consent was obtained at each institution or hospital. The procedure of this study was approved by the Institutional Review Board of the Chiba Cancer Center (CCC7817).

Quantitative reverse transcription–PCR (RT–PCR)

RNA for RT–PCR was extracted from the NB samples using TRizol Reagent (Invitrogen, Carlsbad, CA, USA) and reverse transcribed in 20 μl reactions using SuperScript RNA Amplification System (Invitrogen), in accordance with manufacturer's instructions. For patient samples, quantitative PCR was performed in the Taqman universal master mix (Applied Biosystems, Foster City, CA, USA), which consisted of 1 × mastermix, *hKLF4* (Assay ID Hs00358836_m1) or *GAPDH* (Assay ID Hs02758991_g1) forward and reverse primers, and their probes (Applied Biosystems). For NB cell lines, quantitative PCR was performed using the Cybergreen reaction mix (Applied Biosystems), which consisted of 1 × mastermix, KLF4 forward (5′-TCAGTGGCCGCCACCGTGTCC-3′) and reverse (5′-GTGAAGCTGCAGGTG GAGGGC-3′) primers or 18S forward (5′-CGGCTACCACATCCAAGGA-3′) and reverse (5′-GCTGGAATTACCGCGGCT-3′) primers. The reaction mix (18 μl) was aliquoted into tubes and 1 or 2 μl cDNA was added. Triplicated 20 μl samples and positive and negative controls were placed in a PCR plate and wells were sealed with optical caps. The PCRs were carried out using an ABI Prism 7500 or 7900HT (Applied Biosystems). All Taqman primers and probes were designed by Applied Biosystems. Data were analyzed and processed using Sequence Detector version 1.4 (Applied Biosystems) in accordance with manufacturer's instructions. Primers were optimized and the linearity of the results validated by serial dilution of a plasmid DNA containing h*KLF4* coding sequence. Results were expressed relative to a positive standard (plasmid DNA) that was included in all reaction sets. GADPH or 18S was used as the internal control.

KLF4 expression constructs

Human cDNA for *KLF4* (GenBank or RefSeq NM_004235) that contained the full-length *KLF4* coding region was obtained by PCR and cloned into pFLAG-CMV2 (Sigma-Aldrich, St Louis, MO, USA). For deletion constructs, cDNAs for *KLF4* deletion mutants were obtained by PCR and subcloned into pFLAG-CMV2 (Sigma-Aldrich). KLF4ΔA contains an N-terminal deletion of the transcriptional activation domain and is missing the first 109 amino acid. KLF4ΔDBD lacks the zinc-finger DNA-binding domain (amino acids 350–483). All the plasmids were verified by sequencing.

Cell lines and stable transfectants

Human NB cell lines, SK-N-SH, SH-SY-5Y, SK-N-AS and BE(2)C, from ATCC were grown in MEM or DMEM containing 10% fetal bovine serum, non-essential amino acid and 10 mM sodium pyruvate (Invitrogen). SH-SY-5Y and SK-N-AS have no *MYCN* amplification; SK-N-AS carries mutant p53; BE(2)C has *MYCN* amplification and a p53 mutation. Specific mutations in these NB cells lines are listed in Table 2.

KLF4 overexpressing clones. pFLAG-CMV-KLF4 or pFLAG-CMV construct was transfected into 2×10^5 SH-SY-5Y cells using the Amaxa Nucleofector Kit (Amaxa, Cologne, Germany) according to manufacturer's instructions and grown in DMEM selection medium containing 0.5 μg/ml G418 (Invitrogen). The cloned stable transfectants were tested for FLAG-KLF4 expression using immunoblot analysis with anti-FLAG and anti-KLF4 antibodies (as described below) and used for the subsequent experiments.

KLF4 knockdown clones. MISSION Lentiviral transduction particles expressing non-target shRNA control (SHC002V) or shRNA specifically against KLF4 (TRCN5313) were purchased from Sigma (St Louis, MO, USA). To generate the stable transduced clones, 1×10^5 BE(2)C or SH-SY-5Y cells were seeded into a 35-mm well and transduced with lentiviral transduction particles expressing non-silencing control (NS, 1:100) or shKLF4 (1:20) in the presence of 2 μg/ml polybrene. After 12 h, the virus-containing medium was replaced with fresh culture medium. Four days after the transduction, cells were replated in selection medium, which consisted of full medium with the addition of 2 μg/ml puromycin (Sigma). The stable transduced clones were tested for *KLF4* expression with quantitative RT–PCR.

RT–PCR

Total RNA was isolated from various NB cell lines and stable transfectants by RNeasy mini kit (Qiagen, GmbH, Hilden, Germany) and reverse transcribed in 20 μl reaction system using SuperScript RNA Amplification System (Invitrogen), in accordance with manufacturer's instructions. PCRs were performed using specific primers: human *KLF4* (Forward: 5′-AGAAGGATCTCGGCCAATTT-3′; Reverse: 5′-GGTCTCTCTCCGAGGTAGGG-3′ for 40 cycles; and actin (Forward: 5′-GAATTCATTTTTGAGACCTTCAA-3′; Reverse: 5′-CCGGATCCATCTCTGCCTCGAAGTCCA-3′) for 25 cycles. The estimated sizes of RT–PCR products for h*KLF4* and *actin* were 406 and 306 bp, respectively.

RNA interference

KLF4 siRNA (5′-CCUACACAAAGAGUUCCCAUCUCAA-3′), p21 siRNA (5′-CUUC GACUUUGUCACCGAG-3′) and a non-specific siRNA control (5′-AAUUCUCCGA ACGUGUCACGU-3′) (Qiagen) were used. 0.1 × 106 SK-N-SH cells or SH-SY-5Y stable clones were transfected with KLF4-, p21-specific or non-specific siRNA using LipofectAMINE 2000 (Invitrogen) according to manufacturer's instructions. After 24 h, the cells were subjected to cell proliferation. Knockdown of KLF4 or p21 was confirmed by RT–PCR or western blot.

Immunoblots

To examine the expression of the stable clones and the molecular pathway studies, the G418-resistant clones were isolated after growth in the selection medium for 3 weeks. Cell pellets were collected and then lysed with cell lysis buffer containing 20 mM Tris (pH 7.5), 150 mM NaCl, 1 mM EDTA, 1 mM EGTA, 1% Triton X-100, 2.5 mM sodium pyrophosphate, 1 mM β-glycerophosphate, 1 mM Na_3VO_4, 1 μg/ml leupeptin and 1 mM phenylmethanesulfonyl fluoride. Cell lysates containing 20 μg of total protein were separated on 10% SDS–polyacrylamide gels and blotted onto nitrocellulose membranes. The membranes were then incubated with monoclonal antibodies against FLAG (clone M2, 1:10 000; Santa Cruz Biotechnology, Santa Cruz, CA, USA), cyclin D1 (Cat #Sc-753, 1:1000; Cell Signaling Technology, Beverly, MA, USA), polyclonal $p21^{WAF1/CIP1}$ (12D1, Cat #2947, 1:1000; Cell Signaling Technology), p53 (7F5, Cat #2527, 1:1000; Cell Signaling Technology), pTry118paxillin (1:1000; Cell Signaling Technology Inc.) or paxillin (1:1000; Upstate, Lake Placid, NY, USA). The same membranes were stripped with stripping buffer (100 mM 2-mercaptoethanol, 2% sodium dodecyl sulfate, 62.5 mM Tris–HCl, pH 6.7), blocked and reprobed with a 1:1000 dilution of anti-β-actin monoclonal antibody (Chemicon International, Inc., Temecula, CA, USA) or α-tubulin (Sigma) to ensure equal loading of cell protein per lane. All blots were incubated with 1:5000 dilutions of secondary horseradish peroxidase-conjugated anti-mouse or anti-rabbit antibody (Amersham Pharmacia Biotech., Piscataway, NJ, USA). Antibody-bound proteins were visualized using a chemiluminescence system (Amersham Biosciences, Piscataway, NJ, USA).

Cell proliferation assay

1×10^4 SK-N-SH cells, SH-SY-5Y transfectants or BE(2)C transduced cells were seeded per well in 96-well culture plates for 16 h before addition of BrdU. BrdU (1:1000) was added into the culture for 4 h. The cultures were fixed, blocked and incubated with anti-BrdU antibody. The cell proliferation rate was measured using Cell Proliferation ELISA kit, colorimetric (Roche, Indianapolis, IN, USA). Three independent experiments were performed, and each experiment was in triplicate.

Growth curve assay

1×10^4 BE(2)C transduced clones were seeded in 24-well plate. Cell growth of BE(2)C transduced clones was measured by counting the number of viable cells on days 2, 4, 6 and 8. In brief, cells were harvested and stained with 0.4% trypan blue and the viable cells were counted using hemocytometer. The experiments were performed three times and each in triplicate.

Colony formation assay

One day before transfection, 2×10^5 SK-N-AS cells were seeded onto 35-mm plates. Two micrograms of pFLAG-CMV-KLF4, pFLAG-CMV-KLF4ΔA, pFLAG-CMV-KLF4ΔDBD (FLAG-tagged) or pFLAG-CMV expression vector was co-transfected with 0.2 μg of pcDNA3.1 vector (Promega, Madison, WI, USA) into the cells. After 24 h, cells were seeded onto 100-mm culture dishes in a 1:5 dilution and grown for 2 weeks in medium containing 500 μg/ml G418 (Invitrogen). The neomycin-resistant colonies were fixed with 4% formaldehyde, and colony formation efficiency was examined by Giemsa staining (Sigma-Aldrich).

Soft agar assay

Anchorage-independent growth of KLF4 overexpressing SH-SY-5Y cells was examined using soft agar assay. The base layer consisted of 1% agarose (Invitrogen) in complete SH-SY-5Y medium. 5×10^4 cells were mixed with soft agar composed of 0.4% agarose in complete medium and plated on top of the base layer in 35 mm culture dishes. Soft agar cultures were maintained at 37 °C for an additional 6 weeks and observed for the appearance of colonies with Olympus inverted Microscope CKX41 (Olympus, Hamburg, Germany).

Luciferase reporter assay

$p21^{WAF1/CIP1}$-Luc and p53-Luc reporter constructs were provided by Dr Willison Ching (University of Hong Kong). In total, 500 ng of expression plasmid DNA (pFLAG-CMV-KLF4, pFLAG-CMV-KLF4ΔA, pFLAG-CMV-KLF4ΔDBD or pFLAG-CMV expression vector), 200 ng of reporter constructs (p21-Luc or p53-Luc) and 25 ng of control *Renilla* luciferase construct (TK-RL-Luc) were transfected into 4×10^4 SK-N-AS cells that were plated in a 24-well plate 16 h before the experiment. Cells were harvested according to the Promega Dual Luciferase Reporter assay kit protocol 24 h after transfection. Briefly, cells were washed with PBS, incubated in reporter lysis buffer and bioluminescence was measured using a Microplate Luminometer LB96V (Berthold Technology, Bad Wildbad, Germany). Reporter activity was normalized with *Renilla* luciferase activity to correct for variations in transfection efficiency.

Apoptosis

2×10^5 SK-N-AS cells were transiently transfected with KLF4 expressing plasmids (pFLAG-CMV-KLF4, pFLAG-CMV-KLF4ΔA, pFLAG-CMV-KLF4ΔDBD) or pFLAG-CMV vector as described above. Ninety-six hours after transfection, dead and apoptotic cells were measured using Annexin V-FITC apoptosis detection kit from BD PharMingen (San Jose, CA, USA). Both adherent and floating cells were collected and subjected to Annexin V apoptosis assay. To detect the apoptotic cells, cells were resuspended in 1 × cold binding buffer (10 μmol/l $MgCl_2$, 4% BSA) and stained with FITC-conjugated anti-Annexin V antibody for analysis. Cells were also stained with propidium iodide to detect dead cells. Analyses were done on a FACSCalibur flow cytometer (Becton Dickinson, Franklin Lakes, NJ, USA) using CellQuest software (Becton Dickinson). Cells stained for Annexin V and propidium iodide were apoptotic.

Mouse xenograft studies

A total of 1×10^7 SH-SY-5Y stable transfectants or BE(2)C knockdown clones were injected subcutaneously in the flank of 5- to 6-week-old SCID/Beige mice. The difference in tumor size between the vector control group and the KLF4 overexpressing group was assessed on day 90. The width and length of the tumor were measured and tumor volume was calculated with the equation: width × (width/2) × length. Average volume was then plotted in the bar chart. For BE(2)C knockdown clones, the tumor size was measured for 5 weeks. 1.5×10^6 SH-SY-5Y stable transfectants mixed 1:3 with basement membrane extract (Trevigen, Gaithersburg, MD, USA) were also injected orthotropically into the adrenal fat pad of SCID/Beige mice (5 mice/group) and mice were killed on week 8. Three additional mice injected with KLF4 overexpressing or vector control cells were kept for 100 days. All procedures were approved by the University ethics committee for animal research (CULATR 2215-10). Experiments were terminated when tumors reached a maximum size of 15 mm diameter. After mice were killed, tumors were fixed in 4% paraformaldehyde, then paraffin-embedded and subjected to hematoxylin-eosin staining.

Differentiation assays

Fibromuscular lineage. To induce fibromuscular differentiation of NB cells, BE(2)C non-silencing control or the knockdown clones, cells were grown in media containing 10% serum and 10 μM BrdU (5-bromo-2-deoxyuridine) for 2 weeks. Media containing the drug were renewed three times per week. For immunocytochemistry, 1×10^4 cells were plated into slides coated with poly-lysine (Invitrogen) and cultured for two additional days.

Neural lineage. To induce neural lineage differentiation of NB cells, cells were grown in full media containing 1 μM all-trans-retinoic acid (Sigma) for 4 weeks. Media containing the drug were renewed three times per week and cells were trypsinized at least once per week. A week before harvesting, 5×10^4 cells were plated into a 35-mm-well and neural differentiation was monitored based on the formation of neurite outgrowth on week 4. For each treatment group, a minimum of 9 random fields under × 100 magnification with at least 500 cells in total was photographed for cell counting. The values reported in bar charts represent the mean ± 95% confidence intervals (CIs) of three independent experiments.

Immunocytochemistry

Cells were fixed with 4% paraformaldehyde, stained with mouse anti-SMA (1:500; Sigma) or anti-paxillin (Upstate), and followed by host-appropriate FITC or Texas-Red secondary (Molecular Probes, Invitrogen, Eugene, OR, USA). The F-actin was visualized by tetramethylrhodamine B isothiocyanate (TRITC)-labeled phalloidin (Sigma). Cells were counterstained with DAKO mounting medium containing DAPI to detect nuclei. For SMA staining, a minimum of 9 random fields under × 200 magnification with at least 250 cells in total per 35 mm-well from each treatment group was photographed for cell counting. The values reported in bar charts represent the mean ± 95% CIs of eighteen random fields from two wells and the experiments were repeated three times with four independent stable clones. Cells were photographed using a Nikon Eclipse E600 microscope (Nikon, Melville, NY, USA) with a Sony digital camera DSM1200F (Sony, Tokyo, Japan) under fluorescence illumination.

cDNA microarray and analysis

In all, 2 μg of total RNA was extracted from SH-SY-5Y cells stably transfected with pFLAG-CMV-KLF4 or pFLAG-CMV construct and microarray experiments were performed in triplicates using Human Genome U133 Plus 2.0 GeneChip from Affymetrix. For each array, preprocessing, normalization and analyses were performed identically for all samples, following the standard protocol provided by the manufacturer. Software GeneSpring (Affymetrix) was used for the subsequent data analysis. Genes were considered differentially expressed if the *P*-values were <0.01 and the fold changes were greater than twofold in either direction. Pathway-based analyses were also performed and pathways were considered to be enriched in one group or the other (that is, control or KLF4 overexpressing cells) when one group had two or more genes within that pathway overexpressed than in the other group.

Statistical analysis

Statistical analysis was performed using the SPSS statistics software package (SPSS, Chicago, IL, USA). Statistical comparison for the *KLF4* expression in patients between favorable and unfavorable groups was performed with Mann–Whitney *U*-test. Survival probabilities in various subgroups were estimated according to the Kaplan–Meier method. Survival distributions were compared using log-rank test. The Cox regression model was used to assess the prognostic significance of variables. $P<0.05$ was considered statistically significant.

The differences among multiple transfectants were analyzed with a two-sided unpaired Student's *t*-test using GraphPad Prism 5.00 (GraphPad Software, San Diego, CA, USA). A *P*-value of <0.05 was interpreted to represent a statistically significant difference. Experiments were usually replicated at least three times unless otherwise indicated and data are shown as means with 95% CIs. All statistical tests were two-sided.

CONFLICT OF INTEREST

The authors declare no conflict of interest.

ACKNOWLEDGEMENTS

This study was funded by seed funding grant for basic research from the University of Hong Kong, General Research Grant HKU773909 from the Hong Kong Research Grants Council and research grant from Hong Kong Children Cancer Foundation to ESWN.

REFERENCES

1 Breslow N, McCann B. Statistical estimation of prognosis for children with neuroblastoma. *Cancer Res* 1971; **31**: 2098–2103.
2 Silber JH, Evans AE, Fridman M. Models to predict outcome from childhood neuroblastoma: the role of serum ferritin and tumor histology. *Cancer Res* 1991; **51**: 1426–1433.
3 Brodeur GM, Pritchard J, Berthold F, Carlsen NL, Castel V, Castelberry RP *et al.* Revisions of the international criteria for neuroblastoma diagnosis, staging, and response to treatment. *J Clin Oncol* 1993; **11**: 1466–1477.
4 Hann HW, Evans AE, Siegel SE, Wong KY, Sather H, Dalton A *et al.* Prognostic importance of serum ferritin in patients with Stages III and IV neuroblastoma: the Childrens Cancer Study Group experience. *Cancer Res* 1985; **45**: 2843–2848.
5 Look AT, Hayes FA, Shuster JJ, Douglass EC, Castleberry RP, Bowman LC *et al.* Clinical relevance of tumor cell ploidy and N-myc gene amplification in childhood neuroblastoma: a Pediatric Oncology Group study. *J Clin Oncol* 1991; **9**: 581–591.
6 Seeger RC, Brodeur GM, Sather H, Dalton A, Siegel SE, Wong KY *et al.* Association of multiple copies of the N-myc oncogene with rapid progression of neuroblastomas. *N Engl J Med* 1985; **313**: 1111–1116.
7 Shimada H, Chatten J, Newton Jr WA, Sachs N, Hamoudi AB, Chiba T *et al.* Histopathologic prognostic factors in neuroblastic tumors: definition of subtypes of ganglioneuroblastoma and an age-linked classification of neuroblastomas. *J Natl Cancer Inst* 1984; **73**: 405–416.
8 Shuster JJ, McWilliams NB, Castleberry R, Nitschke R, Smith EI, Altshuler G *et al.* Serum lactate dehydrogenase in childhood neuroblastoma. A Pediatric Oncology Group recursive partitioning study. *Am J Clin Oncol* 1992; **15**: 295–303.
9 Nakagawara A, Arima-Nakagawara M, Scavarda NJ, Azar CG, Cantor AB, Brodeur GM. Association between high levels of expression of the TRK gene and favorable outcome in human neuroblastoma. *N Engl J Med* 1993; **328**: 847–854.
10 Tang XX, Zhao H, Robinson ME, Cohen B, Cnaan A, London W *et al.* Implications of EPHB6, EFNB2, and EFNB3 expressions in human neuroblastoma. *Proc Natl Acad Sci USA* 2000; **97**: 10936–10941.
11 Peterson S, Bogenmann E. The RET and TRKA pathways collaborate to regulate neuroblastoma differentiation. *Oncogene* 2004; **23**: 213–225.
12 Brodeur GM, Minturn JE, Ho R, Simpson AM, Iyer R, Varela CR *et al.* Trk receptor expression and inhibition in neuroblastomas. *Clin Cancer Res* 2009; **15**: 3244–3250.
13 Iraci N, Diolaiti D, Papa A, Porro A, Valli E, Gherardi S *et al.* A SP1/MIZ1/MYCN repression complex recruits HDAC1 at the TRKA and p75NTR promoters and affects neuroblastoma malignancy by inhibiting the cell response to NGF. *Cancer Res* 2011; **71**: 404–412.
14 Janoueix-Lerosey I, Schleiermacher G, Michels E, Mosseri V, Ribeiro A, Lequin D *et al.* Overall genomic pattern is a predictor of outcome in neuroblastoma. *J Clin Oncol* 2009; **27**: 1026–1033.
15 Lastowska M, Cullinane C, Variend S, Cotterill S, Bown N, O'Neill S *et al.* Comprehensive genetic and histopathologic study reveals three types of neuroblastoma tumors. *J Clin Oncol* 2001; **19**: 3080–3090.
16 Michels E, Vandesompele J, De Preter K, Hoebeeck J, Vermeulen J, Schramm A *et al.* ArrayCGH-based classification of neuroblastoma into genomic subgroups. *Genes Chromosomes Cancer* 2007; **46**: 1098–1108.
17 Mosse YP, Diskin SJ, Wasserman N, Rinaldi K, Attiyeh EF, Cole K *et al.* Neuroblastomas have distinct genomic DNA profiles that predict clinical phenotype and regional gene expression. *Genes Chromosomes Cancer* 2007; **46**: 936–949.
18 Ohira M, Oba S, Nakamura Y, Isogai E, Kaneko S, Nakagawa A *et al.* Expression profiling using a tumor-specific cDNA microarray predicts the prognosis of intermediate risk neuroblastomas. *Cancer Cell* 2005; **7**: 337–350.
19 Tomioka N, Oba S, Ohira M, Misra A, Fridlyand J, Ishii S *et al.* Novel risk stratification of patients with neuroblastoma by genomic signature, which is independent of molecular signature. *Oncogene* 2008; **27**: 441–449.
20 Vandesompele J, Baudis M, De Preter K, Van Roy N, Ambros P, Bown N *et al.* Unequivocal delineation of clinicogenetic subgroups and development of a new model for improved outcome prediction in neuroblastoma. *J Clin Oncol* 2005; **23**: 2280–2299.
21 Janoueix-Lerosey I, Schleiermacher G, Delattre O. Molecular pathogenesis of peripheral neuroblastic tumors. *Oncogene* 2010; **29**: 1566–1579.
22 Biagiotti T, D'Amico M, Marzi I, Di Gennaro P, Arcangeli A, Wanke E *et al.* Cell renewing in neuroblastoma: electrophysiological and immunocytochemical characterization of stem cells and derivatives. *Stem Cells* 2006; **24**: 443–453.
23 Marzi I, D'Amico M, Biagiotti T, Giunti S, Carbone MV, Fredducci D *et al.* Purging of the neuroblastoma stem cell compartment and tumor regression on exposure to hypoxia or cytotoxic treatment. *Cancer Res* 2007; **67**: 2402–2407.
24 Rowland BD. Peeper DS. KLF4, p21 and context-dependent opposing forces in cancer. *Nat Rev Cancer* 2006; **6**: 11–23.
25 Dang DT, Chen X, Feng J, Torbenson M, Dang LH, Yang VW. Overexpression of Kruppel-like factor 4 in the human colon cancer cell line RKO leads to reduced tumorigenecity. *Oncogene* 2003; **22**: 3424–3430.
26 Wei D, Gong W, Kanai M, Schlunk C, Wang L, Yao JC *et al.* Drastic down-regulation of Kruppel-like factor 4 expression is critical in human gastric cancer development and progression. *Cancer Res* 2005; **65**: 2746–2754.
27 Foster KW, Ren S, Louro ID, Lobo-Ruppert SM, McKie-Bell P, Grizzle W *et al.* Oncogene expression cloning by retroviral transduction of adenovirus E1A-immortalized rat kidney RK3E cells: transformation of a host with epithelial features by c-MYC and the zinc finger protein GKLF. *Cell Growth Differ* 1999; **10**: 423–434.
28 Foster KW, Liu Z, Nail CD, Li X, Fitzgerald TJ, Bailey SK *et al.* Induction of KLF4 in basal keratinocytes blocks the proliferation-differentiation switch and initiates squamous epithelial dysplasia. *Oncogene* 2005; **24**: 1491–1500.
29 Foster KW, Frost AR, McKie-Bell P, Lin CY, Engler JA, Grizzle WE *et al.* Increase of GKLF messenger RNA and protein expression during progression of breast cancer. *Cancer Res* 2000; **60**: 6488–6495.
30 Yu F, Li J, Chen H, Fu J, Ray S, Huang S *et al.* Kruppel-like factor 4 (KLF4) is required for maintenance of breast cancer stem cells and for cell migration and invasion. *Oncogene* 2011; **30**: 2161–2172.
31 Akaogi K, Nakajima Y, Ito I, Kawasaki S, Oie SH, Murayama A *et al.* KLF4 suppresses estrogen-dependent breast cancer growth by inhibiting the transcriptional activity of ERalpha. *Oncogene* 2009; **28**: 2894–2902.
32 Yori JL, Seachrist DD, Johnson E, Lozada KL, Abdul-Karim FW, Chodosh LA *et al.* Kruppel-like factor 4 inhibits tumorigenic progression and metastasis in a mouse model of breast cancer. *Neoplasia* 2011; **13**: 601–610.
33 Jaubert J, Cheng J, Segre JA. Ectopic expression of kruppel like factor 4 (Klf4) accelerates formation of the epidermal permeability barrier. *Development* 2003; **130**: 2767–2777.
34 Katz JP, Perreault N, Goldstein BG, Lee CS, Labosky PA, Yang VW *et al.* The zinc-finger transcription factor Klf4 is required for terminal differentiation of goblet cells in the colon. *Development* 2002; **129**: 2619–2628.
35 Segre JA, Bauer C, Fuchs E. Klf4 is a transcription factor required for establishing the barrier function of the skin. *Nat Genet* 1999; **22**: 356–360.
36 Feinberg MW, Wara AK, Cao Z, Lebedeva MA, Rosenbauer F, Iwasaki H *et al.* The Kruppel-like factor KLF4 is a critical regulator of monocyte differentiation. *EMBO J* 2007; **26**: 4138–4148.
37 Cordes KR, Sheehy NT, White MP, Berry EC, Morton SU, Muth AN *et al.* miR-145 and miR-143 regulate smooth muscle cell fate and plasticity. *Nature* 2009; **460**: 705–710.
38 Yori JL, Johnson E, Zhou G, Jain MK, Keri RA. Kruppel-like factor 4 inhibits epithelial-to-mesenchymal transition through regulation of E-cadherin gene expression. *J Biol Chem* 2010; **285**: 16854–16863.
39 Chen J, Liu J, Yang J, Chen Y, Ni S, Song H *et al.* BMPs functionally replace Klf4 and support efficient reprogramming of mouse fibroblasts by Oct4 alone. *Cell Res* 2011; **21**: 205–212.
40 Li R, Liang J, Ni S, Zhou T, Qing X, Li H *et al.* A mesenchymal-to-epithelial transition initiates and is required for the nuclear reprogramming of mouse fibroblasts. *Cell Stem Cell* 2010; **7**: 51–63.
41 Okita K, Ichisaka T, Yamanaka S. Generation of germline-competent induced pluripotent stem cells. *Nature* 2007; **448**: 313–317.
42 Ross RA, Spengler BA, Domenech C, Porubcin M, Rettig WJ, Biedler JL. Human neuroblastoma I-type cells are malignant neural crest stem cells. *Cell Growth Differ* 1995; **6**: 449–456.
43 Walton JD, Kattan DR, Thomas SK, Spengler BA, Guo HF, Biedler JL *et al.* Characteristics of stem cells from human neuroblastoma cell lines and in tumors. *Neoplasia* 2004; **6**: 838–845.
44 Acosta S, Lavarino C, Paris R, Garcia I, de Torres C, Rodriguez E *et al.* Comprehensive characterization of neuroblastoma cell line subtypes reveals bilineage potential similar to neural crest stem cells. *BMC Dev Biol* 2009; **9**: 12.
45 Mahller YY, Williams JP, Baird WH, Mitton B, Grossheim J, Saeki Y *et al.* Neuroblastoma cell lines contain pluripotent tumor initiating cells that are susceptible to a targeted oncolytic virus. *PLoS One* 2009; **4**: e4235.
46 Lutz W, Fulda S, Jeremias I, Debatin KM, Schwab M. MycN IFNgamma cooperate in apoptosis of human neuroblastoma cells. *Oncogene* 1998; **17**: 339–346.
47 Chen S, Crawford M, Day RM, Briones VR, Leader JE, Jose PA *et al.* RhoA modulates Smad signaling during transforming growth factor-beta-induced smooth muscle differentiation. *J Biol Chem* 2006; **281**: 1765–1770.

48 McKinsey TA, Olson EN. Toward transcriptional therapies for the failing heart: chemical screens to modulate genes. *J Clin Invest* 2005; **115**: 538–546.
49 Zhang CL, McKinsey TA, Chang S, Antos CL, Hill JA, Olson EN. Class II histone deacetylases act as signal-responsive repressors of cardiac hypertrophy. *Cell* 2002; **110**: 479–488.
50 Iehara T, Hosoi H, Akazawa K, Matsumoto Y, Yamamoto K, Suita S *et al.* MYCN gene amplification is a powerful prognostic factor even in infantile neuroblastoma detected by mass screening. *Br J Cancer* 2006; **94**: 1510–1515.
51 Kaneko M, Tsuchida Y, Mugishima H, Ohnuma N, Yamamoto K, Kawa K *et al.* Intensified chemotherapy increases the survival rates in patients with stage 4 neuroblastoma with MYCN amplification. *J Pediatr Hematol Oncol* 2002; **24**: 613–621.
52 Islam A, Kageyama H, Takada N, Kawamoto T, Takayasu H, Isogai E *et al.* High expression of Survivin, mapped to 17q25, is significantly associated with poor prognostic factors and promotes cell survival in human neuroblastoma. *Oncogene* 2000; **19**: 617–623.
53 Biedler JL, Roffler-Tarlov S, Schachner M, Freedman LS. Multiple neurotransmitter synthesis by human neuroblastoma cell lines and clones. *Cancer Res* 1978; **38**: 3751–3757.
54 Tweddle DA, Malcolm AJ, Cole M, Pearson AD, Lunec J. p53 cellular localization and function in neuroblastoma: evidence for defective G(1) arrest despite WAF1 induction in MYCN-amplified cells. *Am J Pathol* 2001; **158**: 2067–2077.
55 Keshelava N, Zuo JJ, Chen P, Waidyaratne SN, Luna MC, Gomer CJ *et al.* Loss of p53 function confers high-level multidrug resistance in neuroblastoma cell lines. *Cancer Res* 2001; **61**: 6185–6193.
56 Tweddle DA, Malcolm AJ, Bown N, Pearson AD, Lunec J. Evidence for the development of p53 mutations after cytotoxic therapy in a neuroblastoma cell line. *Cancer Res* 2001; **61**: 8–13.
57 Beppu K, Nakamura K, Linehan WM, Rapisarda A, Thiele CJ. Topotecan blocks hypoxia-inducible factor-1alpha and vascular endothelial growth factor expression induced by insulin-like growth factor-I in neuroblastoma cells. *Cancer Res* 2005; **65**: 4775–4781.

Supplementary Information accompanies the paper on the Oncogene website (http://www.nature.com/onc)

Epithelial-mesenchymal transition-related gene expression as a new prognostic marker for neuroblastoma

MEGUMI NOZATO[1], SETSUKO KANEKO[1], AKIRA NAKAGAWARA[2] and HIROAKI KOMURO[3]

[1]Department of Pediatric Surgery, Faculty of Medicine, University of Tsukuba, Tsukuba; [2]Chiba Cancer Center Research Institute, Chiba; [3]Department of Pediatric Surgery, Graduate School of Medicine, University of Tokyo, Tokyo, Japan

Received August 14, 2012; Accepted October 9, 2012

DOI: 10.3892/ijo.2012.1684

Abstract. Neuroblastoma (NB) is a highly metastatic tumor in children. The epithelial-mesenchymal transition (EMT) is an important mechanism for both the initiation of tumor invasion and subsequent metastasis. This study investigated the role of EMT in the progression of NB. Using EMT assays on samples from 11 tumors, we identified 14 genes that were either differentially expressed between tumors of different stages or highly upregulated in NB. Quantitative RT-PCR of these genes was conducted in 96 NB tumors and their expression levels were compared between stages and between tumors with the presence and absence of *MYCN* amplification. The association of survival rate with differential gene expression was investigated. Expression of *KRT19* was significantly decreased in stage 3 or 4 NB as well as stage 4S NB compared with stage 1 or 2 NB. Expression levels of *KRT19* and *ERBB3* were significantly low, and expression levels of *TWST1* and *TCF3* were high in *MYCN*-amplified NB. The patients with low expression of *KRT19* or *ERBB3* showed significantly worse overall survival. Furthermore, the correlation between high invasive ability and low expression of *KRT19* and *ERBB3* was suggested *in vitro* using six NB cell lines. The authors conclude that downregulation of *KRT19* is highly associated with tumor progression in NB and metastasis in localized primary NB and that low expression of *ERBB3* is also associated with progression of NB.

Introduction

Neuroblastoma (NB) is one of the most common pediatric solid tumors, accounting for 15% of all pediatric cancer deaths. It originates from the sympathoadrenal lineage derived from the neural crest. The clinical behavior is markedly heterogeneous (1-3). Most tumors tend to grow aggressively and often have a fatal outcome, but some tumors are favorable and show spontaneous differentiation or regression. The stage of the tumor at diagnosis, the age of the patient and the presence or absence of *MYCN* amplification are the basic parameters used for risk stratification to determine the management and treatment of this disease. Recent progress in chemotherapy has dramatically increased the survival rates of many pediatric cancers; however, advanced stage NB with metastasis, especially those with genomic amplification of the *MYCN* oncogene, are frequently resistant to any therapy and the outcome for patients is still very poor (1-3). Therefore, it is important to know the mechanism of metastasis in NB in order to improve the treatment results.

The epithelial-mesenchymal transition (EMT) is a series of events during which epithelial cells lose many of their epithelial characteristics and take on properties typical of mesenchymal cells. EMT has an important role in the development of many tissues during embryogenesis and similar cell changes are recapitulated during pathological processes, such as fibrosis and cancer. Numerous observations support the idea that EMT has a central role in tumor progression and metastasis (4-7). Cancer cells acquire mesenchymal gene expression patterns and properties, resulting in reduced cell-cell adhesion and the activation of proteolysis and motility. These activities promote tumor invasion and metastasis. EMT is important in the progression of tumor cells acquiring a more invasive, metastatic capacity. In this study, we investigated the role of EMT in the progression of NB in terms of invasiveness and metastasis.

Materials and methods

Tumor samples. Ninety-six primary NBs were obtained from the Department of Pediatric Surgery, University of Tsukuba, and the Division of Biochemistry, Chiba Cancer Center Research Institute, Japan. Patients were aged between 0 months and 18 years at diagnosis (median 16 months). The clinical characteristics of the 96 NBs are shown in Table I.

Cell lines. Six NB cell lines (SK-N-AS, SK-N-DZ, SK-N-SH, GOTO, GANB and TGW) were used for invasion assays. SK-N-SH, SK-N-DZ and SK-N-AS were kindly provided by Toru Sugimoto, Kyoto Prefectural Medical University. TGW and GANB were provided by Chiba Cancer Center. GOTO was

Correspondence to: Professor Hiroaki Komuro, Department of Pediatric Surgery, Graduate School of Medicine, University of Tokyo, 7-3-1 Hongo, Bunkyo-ku, Tokyo 113-8655, Japan
E-mail: komuroh-psu@h.u-tokyo.ac.jp

Key words: neuroblastoma, epithelial-mesenchymal transition, invasive ability, keratin19, ERBB3 (HER3)

Table I. Tumor stages and MYCN amplification of 96 neuroblastomas.

	Stage 1, 2	Stage 4S	Stage 3	Stage 4	Total
MYCN					
Unamplified	22	4	10	15	51
Amplified	2	2	11	30	45
Total	24	6	21	45	96

purchased from American Type Culture Collection (Manassas, VA, USA). These were maintained in Daigo's medium supplemented with 10% fetal bovine serum (BioWest, Nuaille, France) at 37°C in a humidified 5% CO_2 atmosphere.

RNA extraction and cDNA transcription. Total-RNA was prepared from frozen tumor tissue by the guanidine isothiocyanate-phenol method using Isogen (Wako Junyaku Kogyo, Tokyo, Japan) according to the manufacturer's instructions. One microgram of each RNA was reverse transcribed to cDNA with random hexamer primers and transcriptor reverse transcriptase using the Transcriptor First Strand cDNA Synthesis Kit (Roche, USA).

EMT assay. To examine the expression levels of the EMT-related genes, we used an RT^2 Profiler PCR Array for human EMT (SA Biosciences) consisting of quantitative RT-PCR of 84 EMT-related genes. This array coated 96-well microtiter plates and was performed using an ABI Prism 7700 Sequence Detection System (Applied Biosystems, Foster City, CA, USA) according to the following program: 95°C for 10 min, 43 cycles at 95°C for 15 sec and then 60°C for 1 min.

Real-time quantitative RT-PCR. The expression levels of cardesmon 1 (*CALD1*), epidermal growth factor (*EGFR*), desmoplakin (*DSP*), secreted protein acidic and rich in cysteine (*SPARC*), zinc finger E-box-binding homeobox 1 (*ZEB1*), zinc finger E-box-binding homeobox 2 (*ZEB2*), fibronectin 1 (*FN1*), vimentin (*VIM*), keratin 19 (*KRT19*), erythroblastic leukemia viral oncogene homolog (*ERBB3*), regulator of G-protein signaling 2 (*RGS2*), transcription factor 3 (*TCF3*) and *TWIST1* were measured by the ABI Prism 7700 Sequence Detection System (Applied Biosystems) using Universal ProbeLibrary (UPL)-based real-time quantitative RT-PCR (Roche Diagnostics). UPL is based on only 165 short hydrolysis probes of just 8-9 nucleotides, each of which is labeled at the 5' end with FAM and at the 3' end with a dark quencher dye. Human *ACTNB* (β-actin) was used as an internal control gene. The specific primers used are shown in Table II. The UPL probes used were nos. 52, 69, 78, 7, 77, 3, 68, 13, 33, 71, 37, 61, 35, 6 and 64 in UPL for *CALD1, EGFR, DSP, SNAIL2, SPARC, ZEB1, ZEB2, VIM, FN1, KRT19, ERBB3, RGS2, TCF3, TWIST1* and human *ACTNB*, respectively. Each experiment was carried out with each sample in triplicate and repeated twice. The thermal cycling conditions were as follows: 50°C for 2 min, 95°C for 10 min, 40 cycles at 95°C for 15 sec and then 60°C for 1 min. Data from real-time PCR were calculated using the $\Delta\Delta C_t$ method as previously described (8).

Matrigel invasion assay. The invasive ability of NB cell lines was measured using BD Falcon cell culture inserts with an 8-μm pore size PET membrane and 24-well BD BioCoat Matrigel Invasion Chambers (BD Biosciences, Bedford, MA, USA) according to the manufacturer's instructions. NB cell suspensions were adjusted to $1.0x10^5$ cells per well on Matrigel invasion chamber plates and non-matrigel coat invasion chamber (control inserts) and cultured in routine medium in the absence or presence of FBS. After incubation at 37°C under 5% CO_2 for 72 h, the cells that had invaded the chamber and migrated to the lower surface were stained with Diff-Quik (Sysmex, Kobe, Japan) and manually counted under a microscope. The invading cells were stained and counted in

Table II. Sequences of the primers used for PCR.

Gene	Forward primer	Reverse primer
CALD1	5'-GAGCGTCGCAGAGAACTTAGA-3'	5'-TCCTCTGGTAGGCGATTCTTT-3'
EGFR	5'-GCCTTGACTGAGGACAGCA-3'	5'-TTTGGGAACGGACTGGTTTA-3'
DSP	5'-CTTTGCGCCAATTCAATTAAG-3'	5'-CCAGTCCTGAGGTGTATGAGG-3'
SNAIL2	5'-TGGTTGCTTCAAGGACACAT-3'	5'-GTTGCAGTGAGGGCAAGAA-3'
SPARC	5'-GTGCAGAGGAAACCGAAGAG-3'	5'-TGTTTGCAGTGGTGGTTCTG-3'
ZEB1	5'-GGGAGGAGCAGTGAAAGAGA-3'	5'-TTTCTTGCCCTTCCTTTCTG-3'
ZEB2	5'-AAGCCAGGGACAGATCAGC-3'	5'-CCACACTCTGTGCATTTGAACT-3'
VIM	5'-TACAGGAAGCTGCTGGAAGG-3'	5'-ACCAGAGGGAGTGAATCCAG-3'
FN1	5'-GGAAAGTGTCCCTATCTCTGATACC-3'	5'-AATGTTGGTGAATCGCAGGT-3'
KRT19	5'-GCCACTACTACACGACCATCC-3'	5'-CAAACTTGGTTCGGAAGTCAT-3'
ERBB3	5'-CTGATCACCGGCCTCAAT-3'	5'-GGAAGACATTGAGCTTCTCTGG-3'
RGS2	5'-GAAAAGGAAGCTCCAAAAGAGA-3'	5'-TTCTGGGCAGTTGTAAAGCA-3'
TCF3	5'-CTCGGTCATCCTGAACTTGG-3'	5'-TCTCCAACCACACCTGACAC-3'
TWIST1	5'-AAGGCATCACTATGGACTTTCTCT-3'	5'-GCCAGTTTGATCCCAGTATTTT-3'
ACTNB	5'-CCAACCGCGAGAAGATGA-3'	5'-CCAGAGGCGTACAGGGATAG-3'

Table III. Characteristics of 11 neuroblastomas used in EMT assay.

	Stage 1, 2	Stage 4S	Stage 3, 4	Total
MYCN				
Unamplified	1	1	1	3
Amplified	3	2	3	8
Total	4	3	4	11

5 random fields at x100 magnification. The mean number of counted cells was defined as the invasive ability. Each experiment was repeated 3 times.

Statistical analysis. Survival analysis was performed according to the Kaplan-Meier method and the log-rank test. Relative mRNA expression levels were expressed as the mean ± SD. Student's or Welch's t-tests were used to assess the significance of differences between the groups. A p-value of <0.01 was considered statistically significant. This study was approved by the institutional ethics committee for human genome research of the University of Tsukuba (no. 211).

Results

Analysis of EMT-related gene expression in 11 NB tumors using EMT assay. Eleven NB tumors in various stages (Table III) were analyzed by EMT multiple gene profiling microarray. The expressions of 84 EMT-related genes were compared among the 11 tumors using the EMT assay. Seven genes (*CALD1, EGFR, DSP, SNAIL2, SPARC, ZEB1* and *ZEB2*) were found to be differentially expressed between NBs with low stages (stages 1 or 2) and those with high stages (stages 3 or 4). Five genes (*KRT19, ERBB3, RGS2, TCF3* and *TWIST1*) were found to be differentially expressed between *MYCN*-amplified and *MYCN*-non-amplified tumors. These genes and two others highly expressed in NB tumors (*VIM* and *FN1*) were further analyzed in 96 tumors using quantitative PCR.

Correlation of EMT-related gene expression between low and high tumor stages. The expression levels of *ERBB3, RGS2, TCF3, CALD1, EGFR, DSP, SNAIL2, SPARC, ZEB1, ZEB2, VIM* and *FN1* did not show any significant differences between low- and high-stage NB. In contrast, low expression of *KRT19* was significantly associated with high stages of NB (Fig. 1B). *TWIST1* was found to be highly expressed in stage 3 or 4 NB (p=0.011) (Fig. 1A).

Correlation of EMT-related gene expression with metastasis in localized primary tumors. Expression of these EMT-related genes was compared between stage 1 or 2 localized NB and stage 4S NB. Expression of *KRT19* was significantly lower in stage 4S NB, which develops metastasis in localized primary NB (Fig. 1C).

Correlation of EMT-related gene expression with MYCN amplification. Expression of these EMT-related genes was compared between NB with and without *MYCN* amplification.

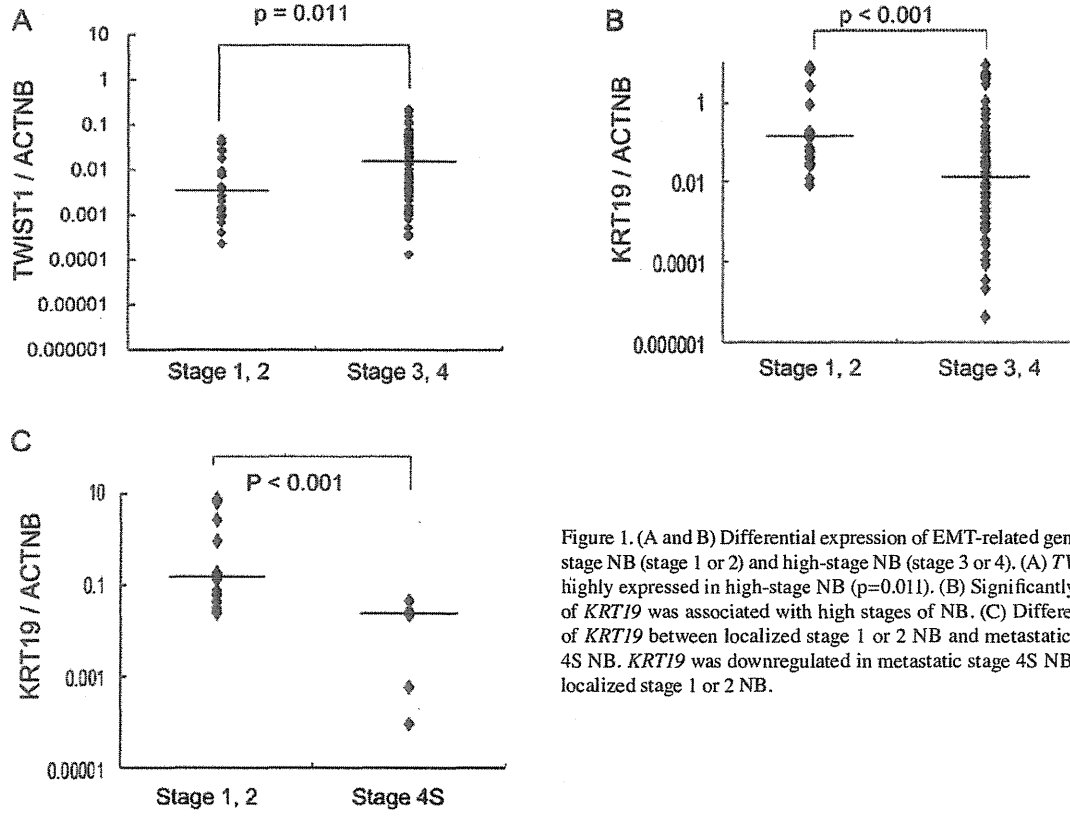

Figure 1. (A and B) Differential expression of EMT-related genes between low-stage NB (stage 1 or 2) and high-stage NB (stage 3 or 4). (A) *TWIST1* was more highly expressed in high-stage NB (p=0.011). (B) Significantly low expression of *KRT19* was associated with high stages of NB. (C) Differential expression of *KRT19* between localized stage 1 or 2 NB and metastatic localized stage 4S NB. *KRT19* was downregulated in metastatic stage 4S NB compared with localized stage 1 or 2 NB.

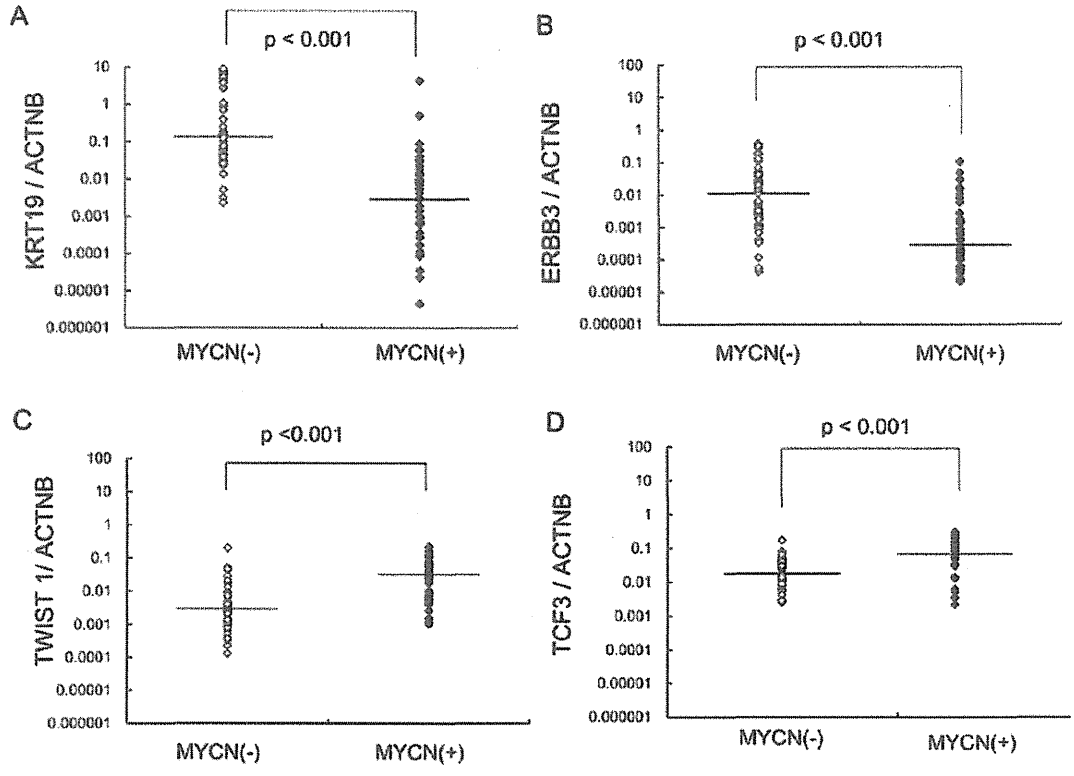

Figure 2. Differential expression of EMT-related genes between *MYCN*-amplified and *MYCN*-unamplified NB. (A and B) Expression of *KRT19* and *ERBB3* was significantly decreased in *MYCN*-amplified NB, (C and D) while expression of *TWIST1* and *TCF3* was significantly increased in *MYCN*-amplified NB. *MYCN*(+), *MYCN* amplification; *MYCN*(-), *MYCN* non-amplification.

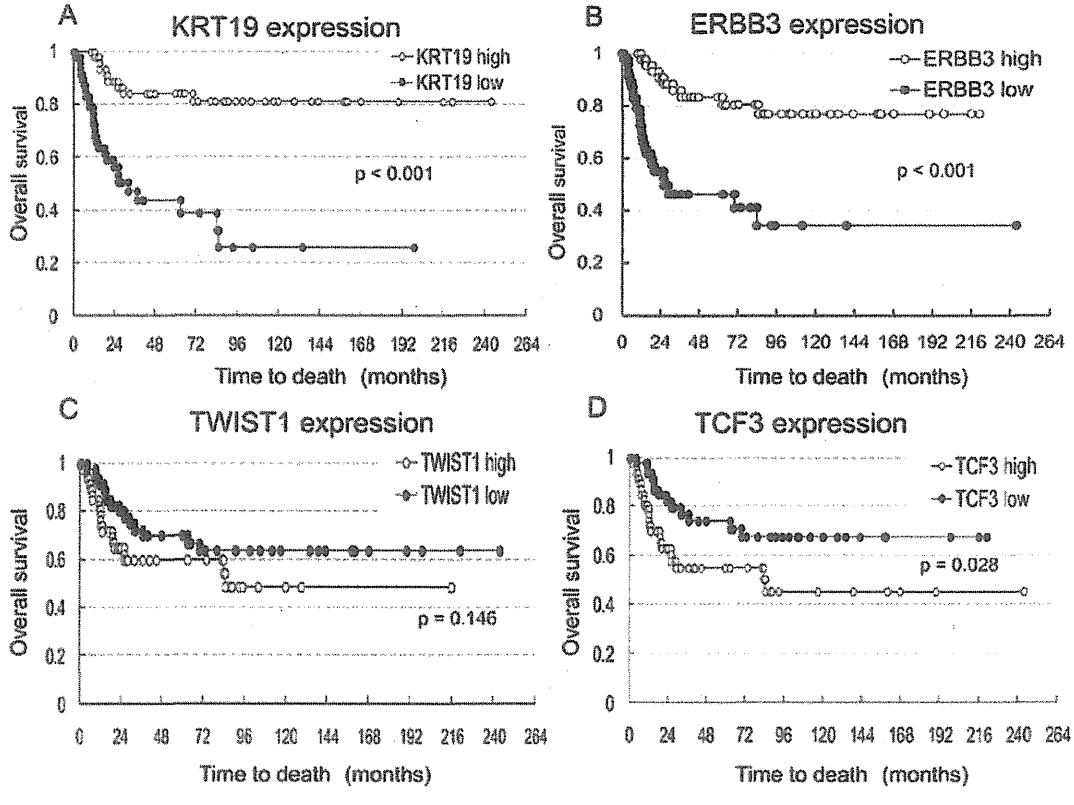

Figure 3. Kaplan-Meier survival analysis of 94 NB patients, stratified by their status of *KRT19*, *ERBB3*, *TWIST1* and *TCF3* gene expression. (A and B) The patients with low expression of *KRT19* or *ERBB3* in tumor tissues had significantly inferior survival compared with those with high expression. (C and D) No significant difference was observed between patients with high and low expression of *TWIST1* and *TCF3* genes.

A

Cell line	Invasion ability (%)	*MYCN* amplification
SK-N-DZ	4.12	+
SK-N-SH	6.75	-
GANB	24.8	+
TGW	45.5	+
SK-N-AS	50.86	-
GOTO	62.14	+

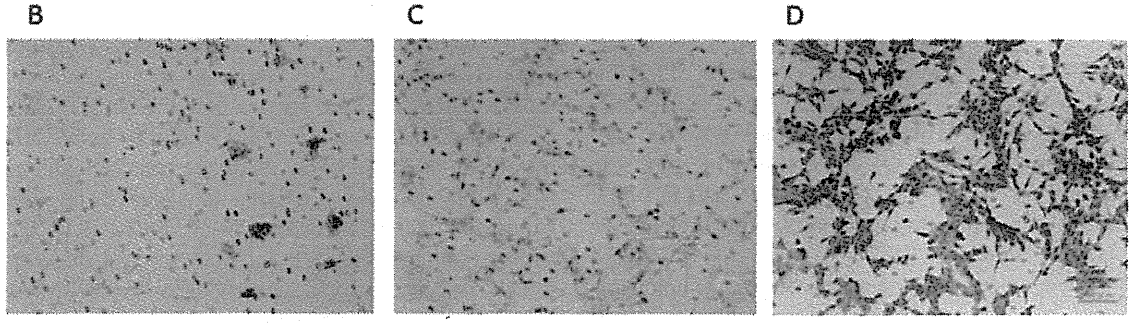

Figure 4. Results of Matrigel invasion assay in 6 NB cell lines. (A) Two cell lines (SK-N-DZ and SK-N-SH) showed low invasive abilities, while the other four cell lines (GANB, TGW, SK-N-AS and GOTO) showed high invasive abilities. (B) SK-N-DZ, (C) SK-N-AS and (D) GOTO cells are shown to be capable of migrating through the matrigel.

Expression of *KRT19* and *ERBB3* was significantly decreased in NB with *MYCN* amplification, while *TCF3* and *TWIST1* expression were increased (Fig. 2). *MYCN*-amplified NB showed significantly lower expression of *KRT19* and *ERBB3* compared with *MYCN*-unamplified NB.

Overall survival rates for tumors with VIM, FN1, KRT19, ERBB3, TCF3 and TWIST1 gene misregulation. Survival analysis was conducted in 94 NB tumors excluding 2 in which NB was not the cause of death. These NBs were divided into two groups: high expressers (47 NBs) and low expressers (47 NBs) of 6 genes (*VIM, FN1, KRT19, ERBB3, TCF3* and *TWIST1*). The median of log-transformed mRNA expression level was used as the cut-off value. Kaplan-Meier survival curves were compared for each gene between tumors with high and low expression (Fig. 3). The graph shows a trend toward increased survival for NB patients with increased *KRT19* or *ERBB3* expression. Expression levels of the other genes (*VIM, FN1, TCF3* and *TWIST1*) were not associated with patient survival.

The correlation of low KRT19 and ERBB3 expression with invasive ability in NB cell lines. A Matrigel invasion assay demonstrated that two cell lines (SK-N-SH and SK-N-DZ) showed significantly reduced invasive ability (6.75 and 4.12%, respectively) while the 4 other cell lines (GANB, TGW, SK-N-AS and GOTO) showed high invasive abilities (24.8, 45.5, 50.86 and 62.1%, respectively) (Fig. 4). The correlation of *KRT19* and *ERBB3* expression with invasive abilities was investigated in the cell lines. The decreased expression of *KRT19* or *ERBB3* was highly correlated with invasiveness in NB cell lines (Fig. 5A and B). SK-N-DZ, with high expression

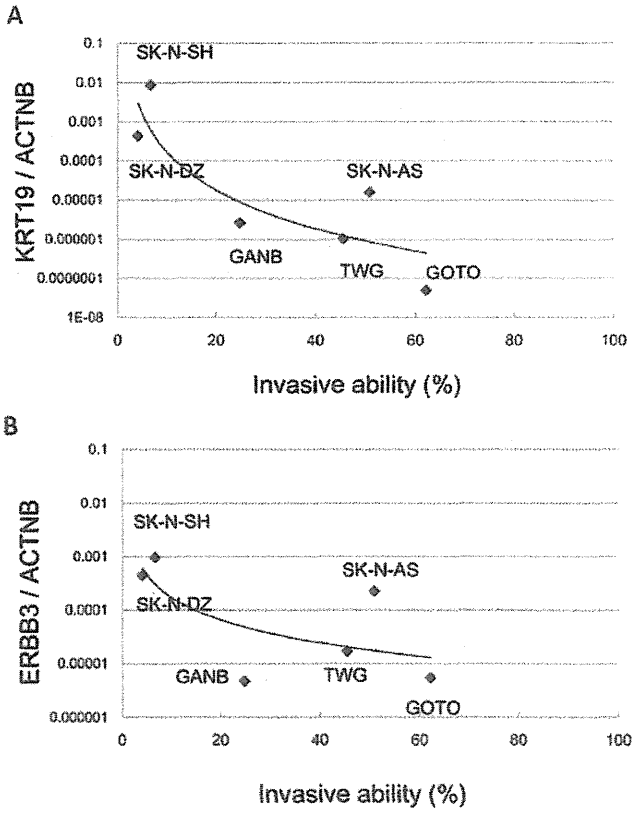

Figure 5. Effects of *ERBB3* and *KRT19* mRNA expression on *in vitro* tumor cell invasiveness. Note the markedly decreased invasive abilities in the cell lines with high expression of (A) *KRT19* and (B) *ERBB3* in comparison to those with low expression.

of *KRT19* and *ERBB3* and *MYCN* amplification, had low invasive ability; while SK-N-AS, with low expression of *KRT19* and *MYCN* non-amplification, showed high invasive ability.

Discussion

In this study, four EMT-related genes (*KRT19*, *ERBB3*, *TWIST1* and *TCF3*) were found to be differentially expressed. Expression of *KRT19* was significantly decreased in high-stage NB compared to low-stage NB (Fig. 1B). Downregulation of *KRT19* gene expression was highly associated with tumor progression in NB. Furthermore, expression of *KRT19* was markedly decreased in NB with *MYCN* amplification. Decreased expression of *KRT19* was found to be significantly associated with poor prognosis (Fig. 3). Interestingly, expression of *KRT19* was significantly decreased in metastatic favorable stage 4S NB compared to localized favorable stage 1 or 2 NB (Fig. 1C). These findings show that decreased expression of *KRT19* is strongly associated with the promotion of metastasis in favorable NB. Keratin is an epithelial marker, and downregulation of keratins is associated with EMT. Dysregulation of keratin expression has long been recognized as a feature of epithelial tumor progression (9). A recent report also demonstrated that expression of *KRT19* mRNA was significantly lower in tumors from patients that have died from NB compared with patients with no evidence of disease, and that low methylation of *KRT19* was associated with a favorable outcome (10). Supporting this, our results demonstrated that low expression of *KRT19* was significantly associated with high tumor stages, *MYCN* amplification and an unfavorable outcome in NB.

TWIST1 is a key regulator of embryogenesis and is also known to be an EMT inducer. *TWIST1* belongs to the basic helix-loop-helix (bHLH) transcription factor family and promotes EMT by repressing the expression of E-cadherin, which leads to disassembly of adherens junctions and increased migratory potential (11). The link between *TWIST1* expression and metastasis is clear and well established (11,12). *TWIST1* is known to be overexpressed in *MYCN*-amplified NB tumors and cell lines and is responsible for the inhibition of the ARF/p53 pathway involved in the MYC-dependent apoptotic response. The cooperation of *TWIST1* and *MYCN* is thought to cause cell transformation and malignant outgrowth (13,14). In this study, *TWIST1* was highly expressed in *MYCN*-amplified NB as well as in high-stage NB. However, the survival rates between patients with low and high expression of *TWIST1* were not significantly different ($p=0.146$), so its utility as a mesenchymal marker may be limited.

TCF3 (E12/E47) is a basic bHLH transcription factor. A previous study implicated *TCF3* as a repressor of E-cadherin promoter activity and demonstrated its involvement in the acquisition and maintenance of the mesenchymal phenotype (15). In this study, high expression of *TCF3* was associated with *MYCN* amplification in NB. Survival rates were not significantly different between patients with high and low expression of *TCF3*.

ERBB3 is a member of the epidermal growth factor receptor (EGFR) family, which is composed of *EGFR*, *ERBB2* (*HER2*), *ERBB3* (*HER3*) and *ERBB4* (*HER4*). Although *ERBB3* lacks an active tyrosine kinase domain, it can heterodimerize with other *ERBB* receptors. Heterodimerization leads to the activation of pathways which lead to cell proliferation or differentiation. The role of EGFR in the proliferation of NB, and the utility of its inhibitors in the treatment of NB, have all been well documented; however, the data remain somewhat contradictory (16,17), as other reports have demonstrated that exposure to EGF can induce apoptosis in NB through the *ERBB2* and *ERBB3* receptors (18-20). Richards *et al* reported that non-EGFR ERBB family members (*ERBB2*, *ERBB3* and *ERBB4*) contributed to NB growth and survival, and that pan-ERBB inhibition, rather than an EGFR specific inhibitor, represents a potential therapeutic target (21). These findings suggest that *ERBB2*, *ERBB3* and *ERBB4* play a significant role in tumor progression of NB, but Gambini *et al* reported that expression of *ERBB2* was not related to tumor progression of NB (22). Although a recent immunohistological study suggested the significance of EGFR family expression as a prognostic factor in NB, showing that *EGFR* and *HER2* expression is found in favorable NB and high expression of *HER4* is found in metastatic NB, the role of HER family members in NB remains interrelated and complex (23). In our study, decreased expression of *ERBB3* was also correlated with *MYCN*-amplified NB and poor survival rate. Several lines of evidence that provide support for the pivotal role of *ERBB3* in human carcinogenesis have emerged in recent years (24). High expression of *ERBB3* in certain human cancers led early to the suggestion that it could be a therapeutic target (25-28), but in some cancer cells the mesenchymal phenotype was found to lose *ERBB3* expression and show resistance to EGFR inhibitors. Epithelial phenotype, however, maintained *ERBB3* expression (29,30). The EMT might decrease the cellular dependency upon EGF signaling by kinase switching; mesenchymal cells might acquire alternative survival signals, thus becoming resistant to EGFR inhibitors (30). Downregulation of *ERBB3* in NB might suggest similar kinase switching during the EMT followed by tumor survival with the loss of EGF dependency.

Next, we investigated the invasive abilities of six NB cell lines using a Matrigel invasion assay to confirm the association of tumor invasiveness with expression of *KRT19* and *ERBB3*. While SK-N-DZ and SK-N-SH cell lines had a low invasive ability (4.12 and 6.75%, respectively), the other cell lines showed a high invasive ability (24.8-62.14%) (Fig. 4). Both cell lines with a low invasive ability had low expression of *KRT19* and *ERBB3* compared with the other cell lines (Fig. 5A and B). Interestingly, SK-N-DZ showed a low invasive ability as expected from high expression levels of *KRT19* and *ERBB3*, although its *MYCN* amplification should give it a high invasive ability. Thus, although *MYCN* gene amplification is the most powerful prognostic factor in NB, the expression levels of *KRT19* or *ERBB3* might become another promising prognostic marker.

Acknowledgements

This study was supported by a Grant-in-Aid for Challenging Exploratory Research from the Japan Society for the Promotion of Science (JSPS) Grant 22659317 (to HK).

References

1. Brodeur GM: Neuroblastoma: biological insights into a clinical enigma. Nat Rev Cancer 3: 203-216, 2003.
2. Maris JM: Recent advances in neuroblastoma. N Engl J Med 362: 2202-2211, 2010.

3. Maris JM: The biologic basis for neuroblastoma heterogeneity and risk stratification. Curr Opin Pediatr 17: 7-13, 2005.
4. Thiery JP and Sleeman JP: Complex networks orchestrate epithelial-mesenchymal transitions. Nat Rev Mol Cell Biol 7: 131-142, 2006.
5. Yang J and Weinberg RA: Epithelial-mesenchymal transition: at the crossroads of development and tumor metastasis. Dev Cell 14: 818-829, 2008.
6. Lee JM, Dedhar S, Kalluri R and Thompson EW: The epithelial-mesenchymal transition: new insights in signaling, development, and disease. J Cell Biol 172: 973-981, 2006.
7. Thiery JP: Epithelial-mesenchymal transitions in tumour progression. Nat Rev Cancer 2: 442-454, 2002.
8. Livak KJ and Schmittgen TD: Analysis of relative gene expression data using real-time quantitative PCR and the $2^{-\Delta\Delta Ct}$ method. Methods 25: 402-408, 2001.
9. Moll R, Franke WW, Schiller DL, Geiger B and Krepler R: The catalog of human cytokeratins: patterns of expression in normal epithelia, tumors and cultured cells. Cell 31: 11-24, 1982.
10. Carén H, Djos A, Nethander M, Sjöberg RM, Kogner P, Enström C, Nilsson S and Martinsson T: Identification of epigenetically regulated genes that predict patient outcome in neuroblastoma. BMC Cancer 11: 66, 2011.
11. Yang J, Mani SA, Donaher JL, Ramaswamy S, Itzykson RA, Come C, Savagner P, Gitelman I, Richardson A and Weinberg RA: Twist, a master regulator of morphogenesis, plays an essential role in tumor metastasis. Cell 117: 927-939, 2004.
12. Karreth F and Tuveson DA: Twist induces an epithelial-mesenchymal transition to facilitate tumor metastasis. Cancer Biol Ther 3: 1058-1059, 2004.
13. Valsesia-Wittmann S, Magdeleine M, Dupasquier S, Garin E, Jallas AC, Combaret V, Krause A, Leissner P and Puisieux A: Oncogenic cooperation between H-Twist and N-Myc overrides failsafe programs in cancer cells. Cancer Cell 6: 625-630, 2004.
14. Puisieux A, Valsesia-Wittmann S and Ansieau S: A twist for survival and cancer progression. Br J Cancer 94: 13-17, 2006.
15. Perez-Moreno MA, Locascio A, Rodrigo I, Dhondt G, Portillo F, Nieto MA and Cano A: A new role for E12/E47 in the repression of E-cadherin expression and epithelial-mesenchymal transitions. J Biol Chem 276: 27424-27431, 2001.
16. Ho R, Minturn JE, Hishiki T, Zhao H, Wang Q, Cnaan A, Maris J, Evans AE and Brodeur GM: Proliferation of human neuroblastomas mediated by the epidermal growth factor receptor. Cancer Res 65: 9868-9875, 2005.
17. Tamura S, Hosoi H, Kuwahara Y, Kikuchi K, Otabe O, Izumi M, Tsuchiya K, Iehara T, Gotoh T and Sugimoto T: Induction of apoptosis by an inhibitor of EGFR in neuroblastoma cells. Biochem Biophys Res Commun 358: 226-232, 2007.
18. Chiu B, Mirkin B and Madonna MB: Epidermal growth factor can induce apoptosis in neuroblastoma. J Pediatr Surg 42: 482-488, 2007.
19. Chiu B, Mirkin B and Madonna MB: Mitogenic and apoptotic actions of epidermal growth factor on neuroblastoma cells are concentration-dependent. J Surg Res 135: 209-212, 2006.
20. Chiu B, Mirkin B and Madonna MB: Novel action of epidermal growth factor on caspase 3 and its potential as a chemotherapeutic adjunct for neuroblastoma. J Pediatr Surg 42: 1389-1395, 2007.
21. Richards KN, Zweidler-McKay PA, Van Roy N, Speleman F, Trevino J, Zage PE and Hughes DP: Signaling of ERBB receptor tyrosine kinases promotes neuroblastoma growth in vitro and in vivo. Cancer 116: 3233-3243, 2010.
22. Gambini C, Sementa AR, Boni L, Marino CE, Croce M, Negri F, Pistoia V, Ferrini S and Corrias MV: Expression of HER2/neu is uncommon in human neuroblastic tumors and is unrelated to tumor progression. Cancer Immunol Immunother 52: 116-120, 2003.
23. Izycka-Swieszewska E, Wozniak A, Drozynska E, Kot J, Grajkowska W, Klepacka T, Perek D, Koltan S, Bien E and Limon J: Expression and significance of HER family receptors in neuroblastic tumors. Clin Exp Metastasis 28: 271-282, 2011.
24. Sithanandam G and Anderson LM: The ERBB3 receptor in cancer and cancer gene therapy. Cancer Gene Therapy 15: 413-448, 2008.
25. Gullick WJ: The c-erbB3/HER3 receptor in human cancer. Cancer Surv 27: 339-349, 1996.
26. Travis A, Pinder SE, Robertson JF, Bell JA, Wencyk P, Gullick WJ, Nicholson RI, Poller DN, Blamey RW, Elston CW and Ellis IO: C-erbB-3 in human breast carcinoma: expression and relation to prognosis and established prognostic indicators. Br J Cancer 74: 229-233, 1996.
27. Sergina NV, Rausch M, Wang D, Blair J, Hann B, Shokat KM and Moasser MM: Escape from HER-family tyrosine kinase inhibitor therapy by the kinase-inactive HER3. Nature 445: 437-441, 2007.
28. Baselga J and Swain SM: Novel anticancer targets: revisiting ERBB2 and discovering ERBB3. Nat Rev Cancer 9: 463-475, 2009.
29. Fuchs BC, Fujii T, Dorfman JD, Goodwin JM, Zhu AX, Lanuti M and Tanabe KK: Epithelial-to-mesenchymal transition and integrin-linked kinase mediate sensitivity to epidermal growth factor receptor inhibition in human hepatoma cells. Cancer Res 68: 2391-2399, 2008.
30. Thomson S, Petti F, Sujka-Kwok I, Epstein D and Haley JD: Kinase switching in mesenchymal-like non-small cell lung cancer lines contributes to EGFR inhibitor resistance through pathway redundancy. Clin Exp Metastasis 25: 843-854, 2008.

The Japanese Journal of Pediatric Hematology/Oncology vol. 49(3): 304–309, 2012

【第53回日本小児血液・がん学会学術集会】ワークショップ2：神経芽腫マススクリーニングのその後

日本小児がん学会と日本神経芽腫研究グループの登録データからみた本邦の神経芽腫実態把握の現況

瀧本　哲也[1]*，池田　　均[2]

[1]国立成育医療研究センター臨床研究センター
[2]獨協医科大学越谷病院小児外科

要　旨

神経芽腫マススクリーニング（MS）休止に際して示された，厚労省検討会の報告書の要請に対処するために必要な神経芽腫の症例把握および研究体制のあり方について，日本小児がん学会全数把握登録（学会登録）と日本神経芽腫研究グループ登録（JNBSG登録）の現状をふまえて考察した．

神経芽腫群腫瘍の登録例数は学会登録では年間約140例，JNBSG登録では約70～80例であり，推定される本邦の症例数のそれぞれ80%，50%前後にすぎない．いずれも臨床研究としての登録であるため，症例の捕捉率に問題があり，また地域ベースの登録ではないためコホートとして追跡することも困難である．一方，地域がん登録は地域ベースでの症例の捕捉率において臨床研究による登録にはるかに優るが，登録内容の面で小児がんに対応しているとは言い難い．

MSの有効性については，MS実施によって年齢や病期別の神経芽腫罹患率や死亡率がどう変化したのかに関する報告が一致していないため，なお議論がある．今後これらのデータを正確に把握し，あわせて神経芽腫MS再開にも利用できるような早期診断法を開発し，適格なリスク判定法とリスクに応じた治療によって神経芽腫の死亡率を減少させるためには，研究グループが地域がん登録と密接に連携して神経芽腫患者を把握する体制を構築し，神経芽腫の生物学的特性の解明や臨床試験などの研究活動を実施していくことが重要である．

キーワード：神経芽腫，マススクリーニング，小児がん登録，地域がん登録
Key words: neuroblastoma, mass screening, childhood cancer registration, population-based cancer registration

神経芽腫のマススクリーニング（MS）は，1985年以降，生後6ヶ月の乳児を対象として全国規模で実施されてきたが，2004年3月をもって，一部の地域を除いて休止された．これは，厚生労働省の「神経芽細胞腫マススクリーニング検査のあり方に関する検討会」（以下，検討会）において，死亡率減少効果が確認できない，不必要な治療による合併症などの不利益が否定できない等の問題点が指摘されたことによる[1]．同報告書ではさらに，神経芽腫の罹患と死亡の正確な把握，新たな検査方法の開発，臨床診断と治療成績の向上のための研究体制の確立などについて，速やかな対応を求めている．

本稿では，この報告書に示された要請に対処するための神経芽腫の症例登録や研究体制のあり方について考察したい．

I　本邦の神経芽腫症例把握の現状

まず，本邦の小児がんを対象とする登録システムのうち，日本小児がん学会小児がん全数把握登録[2]（現：日本小児血液・がん学会「20歳未満に発症する血液疾患と小児がんに関する疫学研究」，以下「学会登録」と略）と日本神経芽腫研究グループ（JNBSG）登録を例として，神経芽腫症例の登録の現状について述べる．

学会登録は，参加施設として本邦の小児がん診療施設の大部分を含み，新規に診断された全ての小児がん患者を登録対象としている．小児固形腫瘍に限れば登録症例数は2008年873例，2009年924例，2010年867例であった．このうち神経芽腫群については年間140例前後の登録がある．学会登録では，これを組織型（神経芽腫，神経節芽腫，神経節腫），性，年齢，都道府県別に集計している（図1～3）．ただし，学会登録の主目的は疾患ごとの発症頻度とその年次推移を把握して，多施設共同臨床研究に役立てることであるため，収集している情報は病名と原発部位を中心とした簡単な項目のみである．症例の捕捉率については，大阪府のがん登録から推定した本邦の小児がん年間症例数と比較すると，神経芽腫（年間症例数150～200例）で80%前後と考えられるほか，他の小児固形腫瘍についても全例を捕捉できているとはいえないものが多い（図4）．

一方，JNBSGは神経芽腫の診断・治療の標準化と全国規模の臨床試験実施を目的として2004年に発足し，2011年6

2012年7月31日受付，2012年7月31日受理
* 別刷請求先：〒157-8535 東京都世田谷区大蔵2-10-1
国立成育医療研究センター臨床研究センター　瀧本哲也
E-mail: takimoto-t@ncchd.go.jp

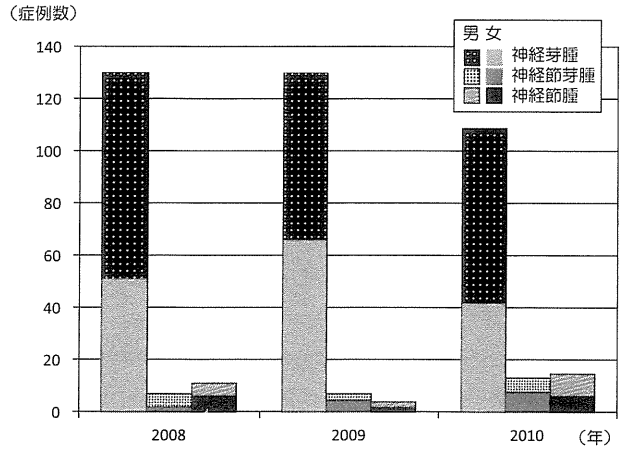

図1　神経芽腫群腫瘍　組織型別・性別登録症例数（日本小児がん学会全数把握登録）

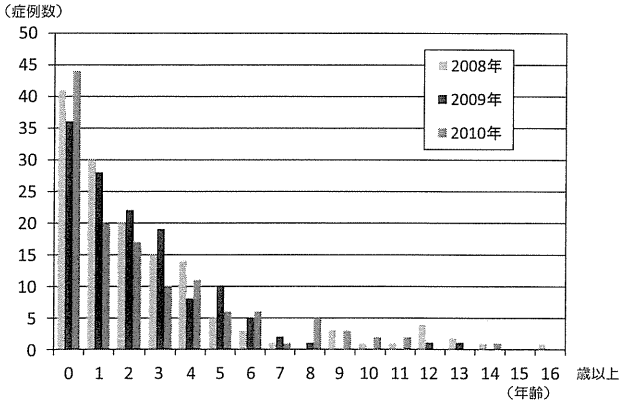

図2　神経芽腫群腫瘍　年齢別症例数（日本小児がん学会全数把握登録）

月の時点で113施設が参加している研究グループである[3]．現在，神経芽腫が疑われた段階で一次登録（JNBSG登録）を行い，匿名化したうえで病理および分子生物学的中央診断を実施し，さらに二次登録として臨床試験あるいは観察研究への登録を行う体制が整備されている．

現在，新規症例の登録は約6～7人/月のペースで，年間70～80人前後となる．JNBSG登録の登録内容は，学会登録のほぼ全ての項目に加えてINSS病期，治療や臨床的転帰などを含み，中央診断の結果や中央診断後の余剰検体の保存状況についてもデータ収集を行っている．これによって臨床試験参加の有無にかかわらず登録された全症例の経過がデータセンターによって追跡され，中央診断で得られた病理学的分類（International Neuroblastoma Pathology Committee分類），mitosis-karyorrhexis index（MKI），MYCN増幅などの予後因子との関連で治療成績を解釈することが可能となっている．このようにJNBSG登録の内容は学会登録に比べてはるかに詳細である一方で，登録症例数は学会登録に比べると60%弱に留まっている．学会登録の捕捉

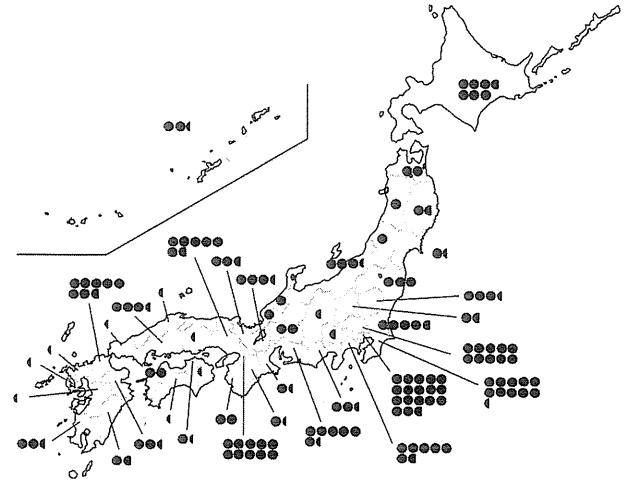

図3　神経芽腫群腫瘍　都道府県別症例数（日本小児がん学会全数把握登録）
3年間の登録症例数の平均を示す．●：年間1例を表す．

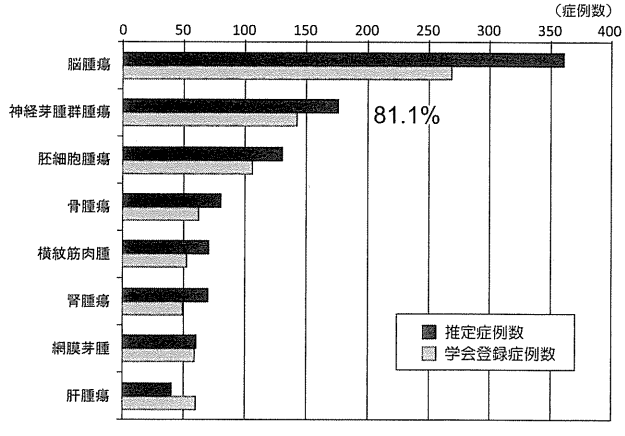

図4　本邦の小児固形腫瘍推定年間症例数と日本小児がん学会全数把握登録症例数

率を約80%とするならば，本邦の神経芽腫のせいぜい半数程度が登録されているにすぎないと考えられる．

II　本邦の小児がん登録の特徴と問題点

本邦では，がんの登録は地域がん登録，院内がん登録，臓器別がん登録の3つに大別される（表1）[4]．このうち地域がん登録は，地域の全がん患者の罹患率や生存率を把握すること，院内がん登録は，医療機関のがん診療の評価を行うことを主な目的としている．これに対して，臓器別がん登録は学会や研究会が中心となって，全国の専門施設を対象として臓器別にがんの詳細な臨床情報を収集するものである．本質的には臨床研究であるため，通常は収集される項目数も前二者に比してはるかに多く，病理学的特徴や進行度，治療法ごとの生存率などを詳細に知ることができ